the atmosphere of argon. The immediately precipitated orange to dark brown crystals were collected and washed with methanol and ether. The propionates were recrystalized from cyclohexane. The trifluoroacetates were used without futher purification.

Electrochemistry. Cyclic voltammetry studies were conducted by using a Hokuto-Denko HB-107A function generator and a HB-104A potentiostat/galvanostat and recorded on a Hitachi 057-1001 X-Y recorder. The electrolysis for ESR measurements and coulometry were performed with a home-made potentiostat, and the current was monitored on a Rikadenki B-161 recorder. The electrolyte solution was CH_2Cl_2 containing n-Bu_4NClO_4 as a supporting electrolyte and 0.1-1 mmol/L of a rhodium complex. Working and auxiliary electrodes were Pt wires for cyclic voltammetry experiments and Au wires for studies of coulometry and electrolysis for ESR. Electrolysis ESR studies were performed with an Allendoerfer type cell with a helix-working electrode[35] and a Maki-Geske type cell.[36]

ESR Spectra. These were obtained on a JEOL PE-2X spectrometer modified with a JEOL ES-SCXA gunn diode microwave unit by using a JES-VT-3A temperature controller or a JES-UCD-2X liquid-nitrogen Dewar bottle. The field sweep was monitored by proton NMR. NMR radio and ESR microwave frequencies were counted on a Takedariken TR-5501 frequency counter equipped with a TR-5023 frequency converter.

Irradiations. Deoxygenated Freon mixture solutions of a rhodium complex were frozen glassily at -196 °C and exposed to ^{60}Co γ-rays at this temperature at a dose rate of 0.04 Mrad/h for up to 40 h. Irradiated samples were annealed at temperatures between -170 to -100 °C in a cold nitrogen gas flow by using a JEOL JES-VT-3A temperature controller.

Simulation of Spectra. Two types of Fortran programs were prepared for simulation of ESR spectra of randomly oriented radicals with an axially symmetric spin Hamiltonian containing quadrupolar couplings. Quadrupolar couplings were included for general application purposes, although these couplings are not applicable to the present radicals. The first program is based on a second-order perturbation solution[37] of the Hamiltonian and takes only the allowed transitions into account. The second program calculates a stick spectrum due to the allowed transitions and the forbidden ones with nonnegligible transition probabilities (threshold, 5%, for example) originating from manually selected nuclei (with large hyperfine couplings and/or quadrupolar couplings) by careful interpolations of eigenvalues and transition moments obtained by solving secular equations for the corresponding spin Hamiltonian at three or four selected magnetic fields. Further splittings due to the remaining nuclei with small hyperfine couplings were treated with a second-order perturbation method. A stick spectrum thus obtained at a given orientation was artificially broadened by an appropriate Gaussian or Lorentzian shape function. Spectra calculated at orientations with an angle increment of 0.5-2° were added together to give a simulated spectrum for randomly oriented radicals. A typical CPU time to calculate a spectrum of a present radical was less than 1 s by the first program and 1-2 s by the second program on a FACOM M200 computer.

Experimental spectra were analyzed by trial-and-error comparisons with simulation spectra calculated with the first program and finally with the second program. The improvement of analyses by the second program was only minor for the present species.

Acknowledgment. We wish to thank Professor G. G. Christoph (Columbus, OH) for supplying X-ray structures of $Rh_2(O_2CMe)_4(PPh_3)_2$ and $Rh_2(O_2CMe)_4(P(OPh)_3)_2$ before publication. We also express our appreciation to Professor J. G. Norman, Jr. (Seattle, WA), for supplying detailed MOs obtained with SCF Xα-SW calculations. We are indebted to Dr. C. Satoko (Okazaki, Japan) for calculations of the Hartree-Fock-Slater AOs of Rh(II) on a HITAC M200 computer at the Institute of Molecular Science. We are grateful to Professor K. Okamoto and Dr. K. Komatsu (Kyoto, Japan) for cyclic voltammetry instruments. Simulations of ESR spectra were performed on a FACOM M200 computer at the Data Processing Center of Kyoto University. Samples were exposed to γ-rays at the Research Laboratory of Radioisotopes of Kyoto University.

(35) Allendoerfer, R. D.; Martinchek, G. A.; Bruckenstein, S. *Anal. Chem.* **1975**, *47*, 890.
(36) Maki, A. H.; Geske, D. H. *J. Am. Chem. Soc.* **1961**, *83*, 1852.
(37) Bleaney, B. *Philos. Mag.* **1951**, *42*, 441.

Mechanism of the Formation of Dihydrogen from the Photoinduced Reactions of Poly(pyridine)ruthenium(II) and Poly(pyridine)rhodium(III) Complexes

S.-F. Chan, Mei Chou, Carol Creutz,* Tadashi Matsubara, and Norman Sutin*

Contribution from the Chemistry Department, Brookhaven National Laboratory, Upton, New York 11973. *Received May 16, 1980*

Abstract: The irradiation of $Ru(bpy)_3^{2+}$, $Rh(bpy)_3^{3+}$, and triethanolamine (TEOA) solutions 10^9 8, 25 °C) with 450 ± 20-nm light yields rhodium(I) (Φ = 0.13 ± 0.02) (units for Φ in mol einstein^{-1} throughout the paper) and dihydrogen (Φ = 0.11 ± 0.02) in the absence and presence of platinum, respectively. A detailed mechanistic scheme has been deduced from the results of continuous- and flash-photolysis experiments: light absorption by $Ru(bpy)_3^{2+}$ gives the excited state $*Ru(bpy)_3^{2+}$ which is oxidized by $Rh(bpy)_3^{3+}$ ($k = 3.9 \times 10^8$ M^{-1} s^{-1}) yielding $Ru(bpy)_3^{3+}$ and $Rh(bpy)_3^{2+}$ with a cage escape yield of 0.15 ± 0.03. Back-reaction of $Ru(bpy)_3^{3+}$ with $Rh(bpy)_3^{2+}$ ($k = 3 \times 10^9$ M^{-1} s^{-1}) is prevented by reduction of $Ru(bpy)_3^{3+}$ by TEOA ($k = 0.2 \times 10^8$ M^{-1} s^{-1}). The oxidized TEOA radical so generated undergoes a TEOA-promoted rearrangement ($k = 0.3 \times 10^7$ M^{-1} s^{-1}) to a reducing radical. The latter reduces $Rh(bpy)_3^{2+}$ so that the net yield for $Rh(bpy)_3^{2+}$ formation is 0.3 ± 0.1. Rate-determining loss of bpy from $Rh(bpy)_3^{2+}$ ($k = 1.0 \pm 0.5$ s^{-1}) is followed by rapid reduction of $Rh(bpy)_2^{2+}$ by $Rh(bpy)_3^{2+}$ ($k = 0.3 \times 10^9$ M^{-1} s^{-1}) giving $Rh(bpy)_3^{3+}$ and Rh(I). In the presence of platinum, H_2 is formed at the expense of Rh(I); catalyzed reaction of Rh(II) with water occurs before disproportionation to Rh(I) can take place. The H_2 quantum yield in this system is limited only by the cage escape of the primary products, the homogeneous and heterogeneous "dark reactions" being very efficient. In the course of this study the electrochemistry of $Rh(bpy)_3^{3+}$, $Rh(phen)_3^{3+}$, and $Rh(bpy)_2(OH)_2^+$ in aqueous solution was investigated, and the quenching of $Ru(bpy)_3^{2+}$ emission by these Rh(III) complexes was characterized.

Introduction

Tris(2,2′-bipyridine)ruthenium(II)[1] ($Ru(bpy)_3^{2+}$) has now proved a useful mediator in the photoreduction of water[2] in both heterogeneous[3-9] and homogeneous systems.[10] For several of the heterogeneous systems studied so far, the following sequence of

(1) For recent reviews see: Sutin, N.; Creutz, C. *Adv. Chem. Ser.* **1978**, *No. 168*, 1; Sutin, N. *J. Photochem.* **1979**, *10*, 19; Whitten, D. G. *Acc. Chem. Res.* **1980**, *13*, 83.
(2) Sutin, N.; Creutz, C. *Pure Appl. Chem.*, in press.
(3) Kalyanasundaram, K.; Kiwi, J.; Grätzel, M. *Helv. Chim. Acta* **1978**, *61*, 2720.

0002-7863/81/1503-369$01.00/0 © 1981 American Chemical Society

events has been implicated. Light absorption by $Ru(bpy)_3^{2+}$ yields the metal-to-ligand charge-transfer excited state $*Ru(bpy)_3^{2+}$ (eq 1). The latter may be oxidized by a second reagent Q to give

$$Ru(bpy)_3^{2+} \xrightarrow{h\nu} *Ru(bpy)_3^{2+} \quad (1)$$

$$*Ru(bpy)_3^{2+} + Q \xrightarrow{k_q} Ru(bpy)_3^{3+} + Q^- \quad (2)$$

$$Ru(bpy)_3^{3+} + Red \xrightarrow{k_s} Red^+ + Ru(bpy)_3^{2+} \quad (3)$$

$$Ru(bpy)_3^{3+} + Q^- \xrightarrow{k_t} Ru(bpy)_3^{2+} + Q \quad (4)$$

$$Q^- + H_2O \xrightarrow{\text{catalyst}} Q + {}^1/_2H_2 + OH^- \quad (5)$$

$Ru(bpy)_3^{3+}$ and Q^- (eq 2). A third reagent Red is added to reduce $Ru(bpy)_3^{3+}$ (eq 3), thus preventing "back-reaction" of Q^- and $Ru(bpy)_3^{3+}$ (eq 4). Subsequent reactions of Q^- with H_2O on the heterogeneous catalyst yield dihydrogen (eq 5). The net reaction is then consumption of 2 equiv of Red for every mole of H_2 formed. The above mechanism has been proposed[6] for the case in which Q is methyl viologen (MV^{2+}, *N,N'*-dimethyl-4,4'-bipyridinium cation) and Red is EDTA (ethylenediaminetetraacetate). An analogous mechanism has been proposed[8] for the tris(2,2'-bipyridine)rhodium(III) ($Rh(bpy)_3^{3+}$), triethanolamine (TEOA) system in which $Rh(bpy)_3^{3+}$ is Q, TEOA is Red, and the catalyst is platinum. Kirch, Lehn, and Sauvage[8b] have described the results of continuous-photolysis experiments on this system and proposed that eq 1–4 are involved but that H_2 evolution arises not from Rh(II) (Q^- in eq 5) but rather from catalyzed reaction of Rh(I) with water. In a recent preliminary account we presented observations bearing out the general mechanism eq 1–5 and indicating that Rh(I) (the product obtained in the absence of platinum) does not reduce water to dihydrogen.[9] In an effort to ascertain the mechanism of dihydrogen formation in the $Ru(bpy)_3^{2+}$, $Rh(bpy)_3^{3+}$, TEOA system, we have made continuous-photolysis studies to determine the nature and yields of the photoproducts and flash-photolysis experiments in order to elucidate the various reaction pathways of the system. In addition, cyclic voltammetry and conventional potentiometry have been used in an attempt to clarify the thermodynamics of rhodium(III), -(II), and -(I) couples relevant to this chemistry. Here we give a detailed account of the continuous- and flash-photolysis studies, as well as the results of the electrochemical measurements. The results of spectrophotometric studies of the bis(2,2'-bipyridine)rhodium(I) species present in aqueous solution under various conditions are described in brief here and will be presented in detail elsewhere.[11]

Experimental Section

Materials. **$[Rh(bpy)_2Cl_2]Cl\cdot 2H_2O$** was prepared according to the method described by Gidney, Gillard, and Heaton.[12] Spectrum (λ_{max} (ϵ)): 311 nm (2.32×10^4 M^{-1} cm^{-1}), 252 (1.90×10^4). Anal.[13] Calcd for $[Rh(bpy)_2Cl_2]Cl\cdot 2H_2O$: Rh, 18.45; C, 43.08; H, 3.62; N, 10.05; Cl, 19.07. Found: Rh, 18.8; C, 43.27; H, 3.89; N, 10.07; Cl, 19.49.

$[Rh(bpy)_3](ClO_4)_3\cdot 3H_2O$ was prepared from $[Rh(bpy)_2Cl_2]Cl$ and bpy following the procedure of DeArmond and Halper.[14] Spectrum (λ_{max} (ϵ)): 320 nm (4.25×10^4 M^{-1} cm^{-1}), 306 (3.93×10^4), 244 (4.10×10^4). Anal.[13] Calcd for $[Rh(bpy)_3](ClO_4)_3\cdot 3H_2O$: Rh, 11.1; Cl, 11.5. Found: Rh, 11.0; Cl, 11.8.

$[Rh(bpy)_2(H_2O)_2](ClO_4)_3\cdot H_2O$ was prepared by a modification of the literature method.[12] $[Rh(bpy)_2Cl_2]Cl$ (0.2 g) was dissolved in 28 mL of 0.17 M sodium hydroxide, and 2 μL of 95% hydrazine hydrate was added to the solution. After the solution had been boiled for 10 min, it became pale green. Heating was continued until the volume of the solution was reduced to ~10 mL. The solution was cooled and filtered, and then concentratd perchloric acid was added dropwise (~0.15 mL) until the light yellow solution became colorless. The volume of the solution was reduced to ~5 mL at room temperature under vacuum, and the solution was chilled overnight. (If, at this stage, the solution was instead heated to reduce its volume, a substantial quantity of $Rh(bpy)_2Cl(H_2O)^{2+}$[12] was found in the product.) The white perchlorate salt was collected on a frit and dried in a vacuum desiccator. Spectrum (λ_{max} (ϵ)) in 0.1 N H_2SO_4: 318 nm (2.83×10^4 M^{-1} cm^{-1}), 305 (2.87×10^4), 243 (2.90×10^4). Spectrum (λ_{max} (ϵ)) in 0.1 N NaOH: 311 nm (2.87×10^4 M^{-1} cm^{-1}), 301 (2.51×10^4), 250 (2.53×10^4). Anal.[13] Calcd for $[Rh(bpy)_2(H_2O)_2](ClO_4)_3\cdot H_2O$: Rh, 13.4; Cl, 13.9. Found: Rh, 13.5; Cl, 13.5.

Triethanolamine (TEOA, Fisher Certified) was purified as follows: 5–10 mL was dissolved in 500 mL of absolute ethanol and the solution was cooled in an ice bath. A chilled solution of ~6 M sulfuric acid in ethanol was then added dropwise to the TEOA solution with stirring until a white solid formed (pH 5–6). The solid was collected on a frit, washed with absolute ethanol, and stored in a vacuum desiccator. Anal. Calcd for $(TEOAH)_2SO_4$: SO_4, 26. Found: SO_4, 24.

The anion-exchange resin used to remove perchlorate ion from solutions of $[Rh(bpy)_3](ClO_4)_3$ and $[Rh(bpy)_2(H_2O)_2](ClO_4)_3$ was obtained as follows. Dowex anion-exchange resin (chloride form, X8, 100–200 mesh) was washed with about three resin volumes each of 1 M hydrochloric acid and water. The resin was then washed with 1 M sodium sulfate until no chloride was detected in the effluent by using silver nitrate. Finally, the resin was washed with water until the effluent from the resin was transparent in the UV (10 resin volumes).

Commercial $Ru(bpy)_3Cl_2\cdot 6H_2O$ (G. F. Smith) was recrystallized from hot water. The preparation and purification of the other ruthenium(II) complexes is described elsewhere.[15] Colloidal platinum was prepared according to the procedure of Rampino and Nord.[16] Other reagents were of the best commercial grade available. Argon was used as blanket gas.

Continuous Photolysis. The photolysis train consisted of a 450-W xenon lamp, focusing lens(es), a high-intensity monochromator or cutoff filters, and a thermostated cell compartment or bath for the photolysis vessel. Solutions not containing platinum were irradiated in 1- or 5-cm cylindrical spectrophotometer cells (2 cm diameter) positioned in the thermostated cell holder behind the monochromator ($I_0 \approx (0.1\text{–}5) \times 10^{-8}$ einstein s^{-1}). The free bpy produced in these photolyses was determined spectrophotometrically; the photolyzed solution was shaken with an equal volume of chloroform, and the absorbance of the chloroform layer at 283 nm ($\epsilon_{bpy} = 1.49 \times 10^4$ M^{-1} cm^{-1}) was determined. The concentration of Rh(I) produced in photolyses at pH 8.1 was determined by scanning the visible spectrum of the product solution ($\epsilon_{eff,515} = 8.7 \times 10^3$ M^{-1} cm^{-1}) against a blank containing the same concentration of $Ru(bpy)_3^{2+}$. Hydrogen evolution from solutions contained in flat-walled Pyrex bottles mounted in a transparent, constant-temperature bath with only cutoff and band-pass filters ($\lambda = 450 \pm 20$ nm) on the lamp ($I_0 = 5 \times 10^{-8}$ einstein s^{-1}) was monitored as follows: 1-mL samples of the 20-mL gas phase above the photolysis solution (20 mL) were taken by syringe at constant pressure from time to time. The gas samples were injected onto a 3-ft column of Poropak Q at 35 °C (argon carrier gas) mounted in a Perkin-Elmer 154 gas chromatograph. In some experiments, H_2 was determined by volumetry; the volume of H_2 (typically 1 mL) produced during a 3-h photolysis was monitored by measuring the volume of mercury displaced in a 1-mL buret at constant pressure. The dark suspension of solid formed during photolysis of solutions containing $Ru(bpy)_3^{2+}$, $Rh(bpy)_3^{3+}$, TEOA, and platinum salts was found to be platinum by atomic absorption spectroscopy. Light intensities were determined by ferrioxalate and by $Co(NH_3)_5Cl^{2+}/Ru(bpy)_3^{2+}$ actinometry. In the latter case, deaerated 0.5 M H_2SO_4 solutions containing $Ru(bpy)_3^{2+}$ and $Co(NH_3)_5Cl^{2+}$ in the ratio 1:20 were photolyzed under

(4) Kiwi, J.; Grätzel, M. *Nature (London)* **1979**, *281*, 657. Kiwi, J.; Grätzel, M. *J. Am. Chem. Soc.* **1979**, *101*, 7214. Kalyanasundaram, K.; Grätzel, M. *Angew. Chem., Int. Ed. Engl.* **1979**, *18*, 701.
(5) Okura, I.; Kim-Thuan, N. *J. Mol. Catal.* **1979**, *5*, 311.
(6) Moradpour, A.; Amouyal, E.; Keller, P.; Kagan, H. *Nouv. J. Chim.* **1978**, *2*, 547.
(7) DeLaive, P. J.; Sullivan, B. P.; Meyer, T. J.; Whitten, D. G. *J. Am. Chem. Soc.* **1979**, *101*, 4007. Durham, B.; Dressick, W. J.; Meyer, T. J. *J. Chem. Soc., Chem. Commun.* **1979**, 381.
(8) (a) Lehn, J.-M.; Sauvage, J.-P. *Nouv. J. Chim.* **1977**, *1*, 449. (b) Kirch, M.; Lehn, J.-M.; Sauvage, J.-P. *Helv. Chim. Acta* **1979**, *62*, 1345.
(9) Brown, G. M.; Chan, S.-F.; Creutz, C.; Schwarz, H. A.; Sutin, N. *J. Am. Chem. Soc.* **1979**, *101*, 7638.
(10) Brown, G. M.; Brunschwig, B. S.; Creutz, C.; Endicott, J. F.; Sutin, N. *J. Am. Chem. Soc.* **1979**, *101*, 1298.
(11) Zipp, A. P.; Chou, M.; Creutz, C.; Sutin, N., manuscript in preparation.
(12) Gidney, P. M.; Gillard, R. D.; Heaton, B. T. *J. Chem. Soc., Dalton Trans.* **1972**, 2621.
(13) Analyses for rhodium were performed by E. Norton using X-ray fluorescence. Analyses for C, H, N, and Cl were carried out by Schwarzkopf.
(14) DeArmond, K.; Halper, W. *J. Phys. Chem.* **1971**, *75*, 3230.
(15) Lin, C.-T.; Böttcher, W.; Chou, M.; Creutz, C.; Sutin, N. *J. Am. Chem. Soc.* **1976**, *98*, 6536.
(16) Rampino, L. D.; Nord, F. F. *J. Am. Chem. Soc.* **1941**, *63*, 2745.

conditions identical with those used in the $Ru(bpy)_3^{2+}$, $Rh(bpy)_3^{3+}$, TEOA system, and the rate of formation of $Ru(bpy)_3^{3+}$ was monitored in the region 450–500 nm. The concentration of $Ru(bpy)_3^{2+}$ in the actinometer was the same as in the $Ru(bpy)_3^{2+}$, $Rh(bpy)_3^{3+}$, TEOA system.

In flash-photolysis experiments the excitation sources were a flash-lamp pumped dye laser[17] and a frequency-doubled neodymium laser.[15,18,19] Quenching rate constants were determined from lifetime measurements or from steady-state emission studies on a spectrofluorimeter.[15]

Electrochemical Measurements. Cyclic voltammetric measurements were performed at 25.0 °C with a Princeton Applied Research 176 potentiostat–galvanostat and a 175 universal programmer. Voltammograms were recorded on a Hewlett-Packard 7000A X-Y recorder when the sweep rates were 200 mV s^{-1} and slower; at faster sweep rates a Tektronix 5115 storage oscilloscope with two 5A21N differential amplifiers was used. The electrochemical cell was a conventional three-electrode type with an aqueous saturated calomel electrode (SCE) as the reference electrode and a platinum wire as the auxiliary electrode. A hanging mercury drop electrode (hmde) was employed as the working electrode in the initial series of experiments; however, there was very strong adsorption of reduction products on the electrode. A pyrolytic graphite working electrode was therefore used in subsequent measurements. Potentials reported in this paper are all vs. the normal hydrogen electrode (NHE) and were calculated by adding 0.242 V to the values measured against the saturated calomel electrode. The potentials have not been corrected for liquid-junction potentials.

Controlled potential coulometry was carried out with the Princeton Applied Research 176 potentiostat–galvanostat. A conventional three-compartment cell was used with graphite rods as the working and auxiliary electrodes and an aqueous saturated calomel electrode as the reference electrode. The cell solution was preelectrolyzed at the applied potential with constant stirring until a steady background current was obtained. The coulometry was performed by adding a known amount of depolarizer to the preelectrolyzed solution and the current–time curve obtained at constant stirring was recorded on a Perkin-Elmer 56 strip-chart recorder. The number of coulombs required for the electrolysis was calculated by integrating the linear ln (current) vs. time plots after compensating for the residual current.

Potentiometric measurements were performed with the pyrolytic graphite electrode and the hmde at 25.0 °C. Since the response time of the graphite electrode was much longer than that of the mercury electrode, the latter was generally used. No adsorption of electroactive species was observed in the potentiometric measurements when no net current was flowing.

Ultraviolet and visible spectra were recorded on a Cary 17 spectrophotometer at room temperature. Solution pH values were measured with a Beckman Research pH meter and an Orion 701 digital pH meter which were calibrated with commercial buffers.

Results and Discussion

Photolysis Products. As has been reported previously,[8,9] photolysis of $Ru(bpy)_3^{2+}$, $Rh(bpy)_3^{3+}$, TEOA solutions at pH 8.1 gives free bpy and a pink-brown solution in the absence of platinum and dihydrogen when K_2PtCl_4 or K_2PtCl_6 has been added. The products responsible for the pink-brown color were shown to be Rh(I) species on the basis of the following experiments. When a 2×10^{-3} M solution of *cis*-$Rh(bpy)_2(OH)_2^+$ in 0.05 M NaOH was reduced at a graphite electrode at −0.96 V, the solution changed from colorless to dark purple. After electrolysis for 8 half-lives (2 h), the number of electrons transferred per *cis*-$Rh(bpy)_2(OH)_2^+$ was calculated to be 1.96 ± 0.05 on the basis of the number of coulombs required for the reduction of the complex. Controlled potential coulometry of 2×10^{-3} M $Rh(bpy)_3^{3+}$ in 0.05 M NaOH at −0.76 V was also attempted. However the Rh(I) produced in the early stages of electrolysis catalyzed the loss of bpy from $Rh(bpy)_3^{3+}$ (over 40 min ~0.8 mol of bpy was released and 0.1 mol of Rh(I) was produced; this effect is discussed further below), and the $Rh(bpy)_2(OH)_2^+$ formed could not be reduced at −0.76 V. In another set of experiments $Rh(bpy)_3^{3+}$ was reduced at an applied potential of −0.96 V and ~2 electrons were consumed per rhodium.

The solution produced upon electrolysis of *cis*-$Rh(bpy)_2(OH)_2^+$ was very air sensitive, with exposure to air resulting in an immediate color change from purple to colorless. The UV spectrum of the air-exposed solution was identical with that of the solution before electrolysis, suggesting that oxidation of the purple species yields *cis*-$Rh(bpy)_2(OH)_2^+$. When the air-oxidized electrolyzed solution was extracted with chloroform, no free bpy was detected in the organic phase. The coulometry indicates a clean two-electron reduction to form a purple Rh(I) product. The fact that no free bpy was found in the electrolyzed solution indicates that two bipyridine ligands are coordinated to the Rh(I). This is also suggested by the quantitative regeneration of the *cis*-$Rh(bpy)_2(OH)_2^+$ spectrum upon air oxidation of the Rh(I) species.

The formal potential for the *cis*-$Rh(bpy)_2(OH)_2^+$/Rh(I) couple was determined as follows: 1.0×10^{-3} M $Rh(bpy)_2(OH)_2^+$ was reduced at a graphite electrode as above. After 5- and 8-min intervals the electrolysis was interrupted and the potential of the solution was measured by using a hmde with SCE as reference. With use of the extents of reduction (16.7 and 38.5%, respectively) calculated from the current–time profile and the potentials measured, the formal potential for the couple is calculated to be −0.45 ± 0.01 V in 0.05 M NaOH and ~−0.23 V in 0.2 M TEOA buffer, pH 8.1, at 25 °C.

The spectrum of the Rh(I) solution depends upon both the pH and the Rh(I) concentration. At high pH the solutions are purple and the position of the absorbance maximum shifts with increasing Rh(I) concentration from ~505 to ~530 nm, with the molar absorptivity at the maximum being independent (to within 10%) of Rh(I) concentration. In the pH range 7–9 the solutions are pink-brown and an additional maximum at ~420 nm is present. Below pH ~6 the solutions are colorless. These spectral changes can be interpreted in terms of pH-dependent equilibria involving several Rh(I) species.[11] At high pH and low Rh(I) concentrations, the predominant Rh(I) species is $Rh(bpy)_2^+$, while at pH <6 this species is protonated to give colorless $Rh(bpy)_2H^{2+}$ or $Rh(bpy)_2(H^-)(H_2O)^{2+}$. At intermediate pH and higher Rh(I) levels the predominant species are the dimers $[Rh(bpy)_2]_2^{2+}$ and $[Rh(bpy)_2]_2H^{3+}$; the latter species are responsible for the pink-brown color of the photolyzed solutions.

The absorption spectrum of the electrolytically produced Rh(I) species (2×10^{-4} M total) present in 0.05 M NaOH features an intense peak at 521 nm, shoulders at ~630 and ~360 nm, and peaks at 297 and 245 nm. When the Rh(I) concentration was determined from the concentration of the radical cation produced upon the addition of the purple solution to excess methyl viologen ($\epsilon_{MV^+} = (1.1 \pm 0.1) \times 10^4$ M^{-1} cm^{-1} at 605 nm[20]), the molar absorptivity for the 521-nm peak was determined to be $(1.1 \pm 0.1) \times 10^4$ M^{-1} cm^{-1}.

To return to the photolysis results, the pink-brown photolysis products are identified as monomeric and dimeric Rh(I) species on the basis of the fact that the spectra of the photolyzed solutions are identical (under comparable conditions) with the spectra of the solutions prepared by the electrochemical (or amalgamated zinc[9]) reduction of *cis*-$Rh(bpy)_2(OH)_2^+$, as described above. On the basis of the above ϵ value of $(1.1 \pm 0.1) \times 10^4$ M^{-1} cm^{-1} at 521 nm for Rh(I) in 0.05 M NaOH, the effective value of ϵ at 515 nm in the 0.20 M TEOA sulfate, pH 8.1 photolysis medium is $(8.7 \pm 1.7) \times 10^3$ M^{-1} cm^{-1} for ~10^{-5} M Rh(I). A quantum yield of 0.13 ± 0.02 is then calculated for Rh(I) formation on the basis of the 515-nm absorbance increases occurring upon irradiation of solutions containing $(0.5–25) \times 10^{-5}$ M $Ru(bpy)_3^{2+}$, 5×10^{-3} M $Rh(bpy)_3^{3+}$, and 0.2 M TEOA sulfate, pH 8.1, at 450 ± 20 nm with I_0 in the range $(0.2–4.0) \times 10^{-9}$ einstein s^{-1}. The absorbance–time profiles exhibit a brief induction period, probably resulting from traces of oxygen in the solutions. From the concentration of free bpy found by extraction into chloroform of a photolysis mixture identical with that described above, the ratio of bipyridine to Rh(I) produced is 0.95 ± 0.10. This result is consistent with the notion that $Rh(bpy)_2^+$ has little affinity for

(17) Hoselton, M. A.; Lin, C.-T.; Schwarz, H. A.; Sutin, N. *J. Am. Chem. Soc.* **1978**, *100*, 2383.
(18) Creutz, C. *Inorg. Chem.* **1978**, *17*, 1046.
(19) Creutz, C.; Chou, M.; Netzel, T. L.; Okumura, M.; Sutin, N. *J. Am. Chem. Soc.* **1980**, *102*, 1309.
(20) Trudinger, P. A. *Anal. Biochem.* **1970**, *36*, 222. Steckhan, E.; Kuwana, T. *Ber. Bunsenges. Phys. Chem.* **1976**, *78*, 253.

Table I. Yield of Free 2,2'-Bipyridine as a Function of the pH of the Photolysis Medium[a]

pH	10^4[bpy], M	pH	10^4[bpy], M
6.9	0.11	10.1	1.4
8.1	0.14	11.0	3.8
9.0	0.36	12.1	20.6
9.1	0.31		

[a] Photolysis of 5×10^{-6} M $Ru(bpy)_3^{2+}$, 5×10^{-3} M $Rh(bpy)_3^{3+}$, and 0.2 M TEOA sulfate adjusted to the pH given was carried out for 20 min in a 5-cm cell at $\lambda = 450 \pm 10$ nm, $I_0 = 3 \times 10^{-9}$ einstein s^{-1}, and 25 °C.

a third bipyridine molecule which is also suggested by the fact that the spectrum of Rh(I) at pH 8.1 is the same in the presence and absence of 10^{-3} M bpy. The photochemical change occurring in the absence of platinum is thus summarized in part by eq 6.

$$Rh(bpy)_3^{3+} + 2e^- = Rh(bpy)_2^+ + bpy \quad (6)$$

In the course of the bpy determinations we found that the bpy/Rh(I) ratio was always high when the photolysis was carried out above pH 9 (see Table I). It will also be recalled that electrolysis of $Rh(bpy)_3^{3+}$ in 0.05 M NaOH at −0.76 V brought about the release of ~0.8 mol of bpy although only ~0.1 mol of Rh(I) was produced. These observations can be understood if Rh(I) catalyzes the equilibration of Rh(III) with bpy and the hydroxide ion (eq 7). In order to investigate this possibility, we

$$Rh(bpy)_3^{3+} + 2OH^- \rightleftharpoons Rh(bpy)_2(OH)_2^+ + bpy \quad (7)$$

added Rh(I) (produced electrolytically) to $Rh(bpy)_3^{3+}$ or to bpy/$Rh(bpy)_2(OH)_2^+$ mixtures at different hydroxide ion concentrations and the compositions of the solutions were determined at various times. When 1.2×10^{-3} M $Rh(bpy)_2(OH)_2^+$ and 1.2×10^{-3} M bpy in 0.1 M TEOA buffer at pH 8.1 was mixed with Rh(I) (final concentration 10^{-4} M), the ultraviolet spectrum (0.1-mm cells) shifted from that of $Rh(bpy)_2(OH)_2^+$ + bpy to that of $Rh(bpy)_3^{3+}$, with the change being largely complete in about 1 h. After ~18 h the solution was extracted with chloroform in order to determine the free bpy level. The composition of the final mixture was thus found to be $\sim 5 \times 10^{-6}$ M bpy and 1.2×10^{-3} M $Rh(bpy)_3^{3+}$ at pH 8.1. Analogous experiments were performed at high pH but starting from 10^{-3} M $Rh(bpy)_3^{3+}$. At 0.1 and 0.01 M NaOH, 10^{-3} M free bpy was present in the solution after ~1 h. (The initial Rh(III) product obtained under these conditions appears dimeric and is converted to *cis*-$Rh(bpy)_2(OH)_2^+$ over ~24 h.) These observations are consistent with a model in which the equilibrium constant for reaction 7 is $\sim 10^{-3}$ M^{-1}, and the equilibrium is attained within a few hours in the presence of 10^{-4} M Rh(I). The high bpy yields found after photolysis of solutions at high pH thus arise because Rh(I) formed photochemically catalyzes the loss of bpy from the $Rh(bpy)_3^{3+}$ and the equilibrium (eq 7) lies to the right at high pH. By contrast, reaction 7 lies to the left under photolysis conditions at pH 8 and below.

As noted earlier,[8,9] photolysis of $Ru(bpy)_3^{2+}$, $Rh(bpy)_3^{3+}$, and K_2PtCl_4 (or K_2PtCl_6) yields dihydrogen. The formation of H_2 exhibits an induction period of about 20–30 min. Before irradiation the solutions are orange and transparent: as irradiation proceeds they become brown and then turbid. Free bpy is also produced.[9] Centrifugation of an extensively photolyzed solution yields a fine purple solid (λ_{max} of suspension is 585 nm) which is pure platinum by analysis. Evidently Pt(II) or -(IV) is reduced to Pt(0) by Rh(I) or Rh(II) in the course of photolysis. Two additional lines of evidence suggest that Pt(0) is the active catalyst for dihydrogen production. First, if K_2PtCl_4 is omitted while colloidal Pt(0)[16] is added, dihydrogen is formed with no induction period. Secondly, the length of the induction period for 3×10^{-4} M K_2PtCl_4 corresponds to formation of 3×10^{-4} M Rh(I) (in the absence of K_2PtCl_4).[9] The Pt(0) could be formed in the reduction of $PtCl_4^{2-}$ by either $Rh(bpy)_2^+$ or $Rh(bpy)_3^{2+}$; the former reductant is more likely since it provides an explanation for the accumulation of free bpy in the solution at early photolysis times.

Table II. Hydrogen Quantum Yields Obtained for 450 ± 20-nm Irradiation of $Ru(bpy)_3^{2+}$, $Rh(bpy)_3^{3+}$, TEOA, and K_2PtCl_4 Solutions at 25 °C[a]

pH	$10^4 \times$ $[Ru(bpy)_3^{2+}]$, M	$10^3 \times$ $[Rh(bpy)_3^{3+}]$, M	$10^3 \times$ $[Rh(bpy)_2(OH)_2^+]$, M	[TEOA], M	Φ_{H_2},[b] mol einstein^{-1}
8.1	5.0	2.0		0.20	0.11[c]
8.1	3.5	2.0		0.20	0.10
8.1	2.0	2.0		0.20	0.11
8.1	1.2	2.0		0.20	0.11
8.1	1.2	2.0		0.20	0.09[d]
8.1	0.50	5.0		0.20	0.12
8.1	0.20	2.0		0.20	0.11
8.1	0.50	5.0	0.50	0.20	0.009
8.1	2.0	5.0	1.30	0.20	0.000
8.1	2.0	2.0	35.0	0.20	0.005[e]
7.0	2.0	2.0		0.40	0.12
7.0	2.0	2.0		0.40	0.10[d]
5.0	3.0	2.0		0.40	0.02[f]
5.0	2.0	2.0		[g]	0.04[f]

[a] The K_2PtCl_4 concentrations were 2.8×10^{-4} M unless otherwise noted. [b] The quantum yields have been corrected for the fraction quenched and for the fraction of the incident light absorbed by $Ru(bpy)_3^{2+}$. [c] The K_2PtCl_4 concentration was 1.0×10^{-4} M. [d] 3.0×10^{-3} M bpy was added before the photolysis. [e] The K_2PtCl_4 concentration was 2.0×10^{-4} M. [f] No K_2PtCl_4 was added. [g] The TEOA was replaced by 0.2 M Na_2H_2EDTA.

Quantum yields for H_2 production were obtained from the maximum H_2 evolution rates (observed immediately after the induction period). The dependence of the hydrogen quantum yield on pH, $Ru(bpy)_3^{2+}$, added bpy, added $Rh(bpy)_2(OH)_2^+$, and TEOA concentrations is shown in Table II. The tabulated values were corrected for light scattering by the platinum suspension by using eq 8 where $\Phi_{H_2}(app)$ is the measured quantum yield (corrected for the fraction quenched), $A_d(\lambda)$ and $A_{Pt}(\lambda)$ are the absorbance of the $Ru(bpy)_3^{2+}$ and Pt(0), respectively (the latter was measured after 2–3-h photolysis time), and $I_0(\lambda)$ is the number of incident photons cm^{-2} s^{-1} per unit wavelength interval. The correction was appreciable at the lowest $Ru(bpy)_3^{2+}$ concentration used but amounted to less than 10% at the higher $Ru(bpy)_3^{2+}$ concentrations. It is evident from Table II that the maximal quantum yield for H_2 is 0.11 ± 0.02 under a range of conditions.

$$\frac{\Phi_{H_2}}{\Phi_{H_2}(app)} = \frac{\sum_\lambda I_0(\lambda)[1 - 10^{-A_d(\lambda)}]}{\sum_\lambda I_0(\lambda)[1 - 10^{-(A_d(\lambda) + A_{Pt}(\lambda))}] \dfrac{A_d(\lambda)}{A_d(\lambda) + A_{Pt}(\lambda)}} \quad (8)$$

Kirch, Lehn, and Sauvage report that added bpy substantially increases the H_2 evolution rate.[8b] We find that the maximum Φ_{H_2} is slightly *smaller* (0.09 ± 0.02) in the presence of bpy but that the rate of H_2 formation is constant for a longer time (>3 h) when bpy is added. The lowered Φ_{H_2} may result from a decreased cage escape yield (vide infra) since added bpy also lowers the Rh(I) quantum yield by ~25%. The increased stability of the mixture during photolysis could result from the fact that the dissociation of $Rh(bpy)_3^{3+}$ to $Rh(bpy)_2(OH)_2^+$ (vide infra) is suppressed by added bpy or from some effect on the properties of the active Pt(0) species. Observations made for solutions containing 5×10^{-3} M zinc sulfate may have a related origin: Rh(I) was found to accumulate, and the rate of H_2 formation dropped much sooner than in the absence of Zn^{2+}. Since Zn^{2+} binds bpy, it lowers the free bpy concentration below the usual level of $\sim 10^{-4}$ M. In a few experiments, 2×10^{-3} M perdeuteriobipyridine was added to the usual K_2PtCl_4 mixture before photolysis. The photolysis mixture was extracted with $CHCl_3$ after ~30-min irradiation (before H_2 evolution commenced), and the isotopic composition of the bpy was determined by mass spectrometry. Greater than 50% scrambling with the bpy bound to $Rh(bpy)_3^{3+}$ had occurred. This scrambling was probably catalyzed by the photoproduced Rh(I).

The dependence of the H_2 yield on platinum concentration was investigated in some early experiments by using K_2PtCl_6 instead

Table III. Quenching of the Emission of Poly(pyridine)ruthenium(II) Complexes by Rhodium(III) Complexes at 25 °C and 0.5 M Ionic Strength

donor	$*E^{\circ}$,[a] V	$10^{-8}k_q$, M^{-1} s^{-1}			
		$Rh(bpy)_3^{3+}$ [b]	$Rh(phen)_3^{3+}$ [d]	$Rh(bpy)_2(H_2O)_2^{3+}$ [d]	$Rh(bpy)_2(OH)_2^{+}$ [c]
$*Ru(5\text{-}Cl(phen))_3^{2+}$	−0.77	4.1 (2.8)	5.7	2.9	0.11
$*Ru(bpy)_3^{2+}$	−0.84	6.2 (3.7)[e]	6.8	4.4	0.12
$*Ru(phen)_3^{2+}$	−0.87	9.9 (7.1)	11.6	6.5	0.12
$*Ru(4,4'\text{-}(CH_3)_2(bpy))_3^{2+}$	−0.94	11.4 (7.7)	13.7	7.8	0.18
$*Ru(4,7\text{-}(CH_3)_2(phen))_3^{2+}$	−1.01	12.5 (9.9)	14.7	13.9	0.25

[a] Reference 1. [b] In 0.5 M H_2SO_4; the numbers in parentheses are the rate constants for quenching in 0.5 M NaOH. [c] In 0.5 M NaOH. [d] In 0.5 M H_2SO_4. [e] The quenching rate constant is 3.9×10^8 M^{-1} s^{-1} at 25 °C in 0.17 M Na_2SO_4.

of K_2PtCl_4. After 1-h irradiation the spectra of the solutions (entry 6 in Table II) were scanned and the gas above the solutions was sampled. At low $PtCl_6^{2-}$, both H_2 and Rh(I) were produced ([K_2PtCl_6], μmol of H_2, μmol of Rh(I)): 0 M, 0, 2.2; 0.1×10^{-4} M, 0.1, 1.7; 0.3×10^{-4} M, 0.9, 1.4; 1.0×10^{-4} M, 1.2, <0.5. Unfortunately these data cannot be compared on a quantitative basis since (1) at low platinum, Rh(I) accumulates and acts as an "inner filter", thus lowering light absorption by $Ru(bpy)_3^{2+}$, and (2) at high platinum, light scattering by the platinum suspension has a similar effect. These data, do, however, demonstrate unequivocally that H_2 and Rh(I) may coexist on a rather long time scale in the presence of the catalyst and so suggest that the two products form in parallel from a common precursor, that is, that Rh(I) does not rapidly (or at all) reduce water to H_2 in the presence of Pt(0). This hypothesis was tested directly by stirring electrochemically generated Rh(I) with colloidal platinum at room temperature under a variety of conditions and assaying the gas above the solution for hydrogen. Less than 0.2 μmol of H_2 was found in each of the following experiments (conditions, time elapsed): (a) 20 mL of 4×10^{-4} M $Rh(bpy)_2^{+}$ (8.0 μmol)/0.4 M TEOA sulfate/pH 7.0/5×10^{-3} M bpy, 1 and 18 h; (b) as in a and 1×10^{-3} M $Rh(bpy)_3^{3+}$, 3 h; (c) as in a but pH 8.0, 3 and 18 h; (d) 20 mL of 4×10^{-4} M $Rh(bpy)_2^{+}$/0.1 N H_2SO_4, 18 h; (e) 20 mL of 4×10^{-4} M $Rh(bpy)_2^{+}$/0.1 M acetic acid–sodium acetate/pH 5, 18 h. The results for experiment a must be reconciled with the fact that $Rh(bpy)_3^{+}$ *is* a strong enough reductant to reduce water at pH 7.0 (vide infra). Possibly no H_2 is formed because the affinity of $Rh(bpy)_2^{+}$ for bpy is so small that the concentration of $Rh(bpy)_3^{+}$ is negligible at 5×10^{-3} M bpy. Photolysis of electrogenerated Rh(I) in pH 8 TEOA sulfate (λ = 450 ± 20 nm) yielded no detectable H_2.

In accord with Kirch, Lehn, and Sauvage,[8b] we find that H_2 is produced in the absence of added platinum in acidic EDTA (or TEOA) solutions: for irradiation of 3.0×10^{-4} M $Ru(bpy)_3^{2+}$, 2.0×10^{-3} M $Rh(bpy)_3^{3+}$, and 0.2 M Na_2H_2EDTA, pH 5, the quantum yield of H_2 is 0.04. A long induction period was observed and rhodium(I) and free bpy (Φ = 0.012 and 0.011, respectively) were also detected in the photolyzed solution. This platinum-free system is presently under further investigation.[21]

In summary, the products of the continuous photolysis at pH 8 are Rh(I) and H_2, in the absence and presence of platinum, respectively. In addition, triethanolamine (and light) is (are) consumed under both sets of conditions. Although not studied in this work, the triethanolamine oxidation products are glycol aldehyde and diethanolamine so that net energy storage is accomplished.[8] The quantum yield for the formation of Rh(I) and free bpy in the absence of added platinum is 0.13 ± 0.02, while the quantum yield for the formation of H_2 in the presence of platinum is 0.11 ± 0.02. No H_2 was found to result from the oxidation of Rh(I) by water at pH 1–8 even after 24 h (typical photolysis times were 1–3 h). The mechanistic implications of these observations are pursued in the following sections.

(21) Preliminary observations (D. Mahajan, umpublished work) indicate that H_2 may derive from a Rh(III) dihydride generated via reduction of Rh(I) by $Rh(bpy)_3^{2+}$. Homogeneous hydrogen formation has also been reported to result from UV photolysis of *cis*-$Rh(bpy)_2Cl_2^{+}$ in the presence of TEOA: Kalyanasundaram, K. *Nouv. J. Chim.* **1979**, *3*, 511.

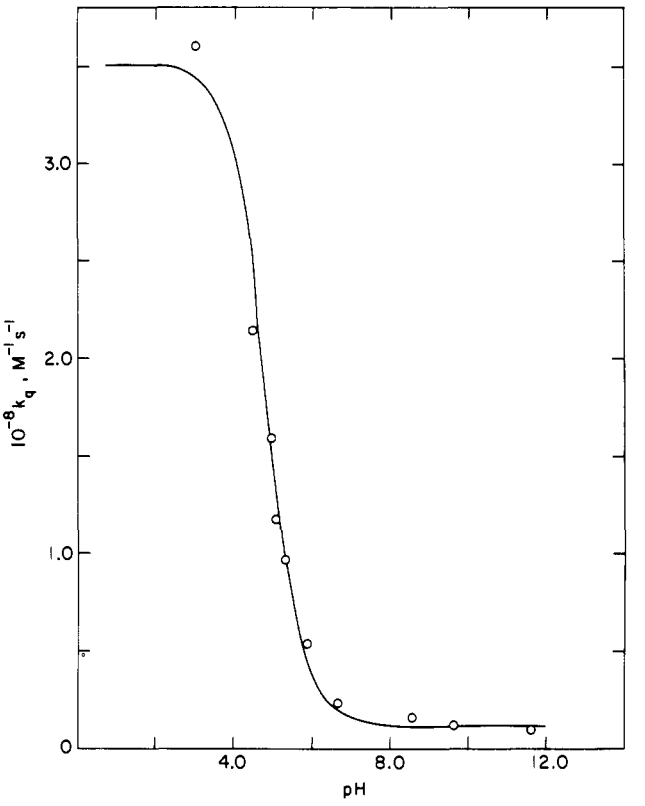

Figure 1. Plot of the rate constants for the quenching of $Ru(bpy)_3^{2+}$ emission by $Rh(bpy)_2(H_2O)_2^{3+}$ as a function of pH at 0.5 M ionic strength and 25 °C. The solid curve was calculated from eq 11.

Quenching Constants. Tris(1,10-phenanthroline)- and tris(2,2′-bipyridine)rhodium(III) quench the RuL_3^{2+} excited states (L = 2,2′-bipyridine, 5-chlorophenanthroline, etc.) with rate constants exceeding 10^8 M^{-1} s^{-1}, as shown in Table III. Rate constants for quenching of $*RuL_3^{2+}$ emission by $Rh(bpy)_2(H_2O)_2^{3+}$ are also tabulated in Table III. While, in acid, $Rh(bpy)_2(H_2O)_2^{3+}$ is nearly as effective a quencher as $Rh(bpy)_3^{3+}$, its quenching efficiency drops sharply at higher pH. This is shown for $*Ru(bpy)_3^{2+}$ in Figure 1 in which k_q is plotted vs. pH. The quenching pattern is due to the fact that the dominant form of the Rh(III) changes according to eq 9 and 10 as the pH of the

$$Rh(bpy)_2(H_2O)_2^{3+} = Rh(bpy)_2(H_2O)(OH)^{2+} + H^{+} \quad K_{a1} \quad (9)$$

$$Rh(bpy)_2(H_2O)(OH)^{2+} = Rh(bpy)_2(OH)_2^{+} + H^{+} \quad K_{a2} \quad (10)$$

medium increases. The pK_a values of $Rh(bpy)_2(H_2O)_2^{3+}$ and $Rh(bpy)_2(H_2O)(OH)^{2+}$ were determined from pH titration of 0.1 M $Rh(bpy)_2(H_2O)_2^{3+}$ dissolved in 0.5 M potassium trifluoromethanesulfonate with 1.0 M NaOH to be 4.8 and 6.8, respectively. These are in reasonably good agreement with the pK_a values 4.4 and 6.4 for eq 9 and 10, respectively, reported in ref 8. Taking reactions 9 and 10 into account, the observed values of k_q (Figure

Table IV. Rate Constants for Quenching of $*Ru(bpy)_3^{2+}$ at 25 °C in Aqueous Solutions

quencher	conditions	k_q, M^{-1} s^{-1}
$PtCl_6^{2-}$	0.17 M Na_2SO_4	$(7.2 \pm 0.7) \times 10^9$
$PtCl_4^{2-}$	0.17 M Na_2SO_4	2.6×10^9
TEOA	μ = 0.5 M (Na_2SO_4)	$<2 \times 10^5$
Rh(I)	μ = 0.5 M (Na_2SO_4), pH 8	$\leq 1 \times 10^9$
$Rh(bpy)_2Cl(H_2O)^{2+}$	0.5 M H_2SO_4	$(1.0 \pm 0.1) \times 10^9$
$Rh(bpy)_2Cl(OH)^+$	0.5 M NaOH	$(0.4 \pm 0.1) \times 10^9$

1) are related to the rate constants for quenching by $Rh(bpy)_2(H_2O)_2^{3+}$ and its conjugate base forms by eq 11. The solid curve

$$k_q = \frac{k_a + k_b K_{a1}/[H^+] + k_c K_{a1} K_{a2}/[H^+]^2}{1 + K_{a1}/[H^+] + K_{a1}K_{a2}/[H^+]^2} \quad (11)$$

in the figure was calculated from eq 11 where k_a, k_b, and k_c are the rate constants for quenching by $Rh(bpy)_2(H_2O)_2^{3+}$ (3.50×10^8 M^{-1} s^{-1}), $Rh(bpy)_2(H_2O)(OH)^{2+}$ (0.20×10^8 M^{-1} s^{-1}), and $Rh(bpy)_2(OH)_2^+$ (0.12×10^8 M^{-1} s^{-1}). (The above value of k_q is slightly lower than the value in 0.5 M H_2SO_4 reported in Table III; this is presumably due to a medium effect: note that quenching by $Rh(bpy)_3^{3+}$ (Table III) shows a modest catalysis by bisulfate ion.) Rate constants for quenching of other $*RuL_3^{2+}$ species by $Rh(bpy)_2(OH)_2^+$ are summarized in the last column of Table III and are at least 1 order of magnitude smaller than the $Rh(bpy)_2(H_2O)_2^{3+}$ quenching rate constants.

Quenching and flash-photolysis studies of several other species were made in order to sort out their roles in the photochemistry of the system. These results are summarized in Table IV. Both $PtCl_6^{4-}$ and $PtCl_6^{2-}$ quench $*Ru(bpy)_3^{2+}$ very rapidly,[9,22,23] but neither gives rise to redox products.[9] Thus in terms of *photochemical* events they need only be considered because they introduce small losses of $*Ru(bpy)_3^{2+}$ (due to their quenching) early in the photolyses. No quenching and no products were observed for TEOA so that it also plays a role in only the "dark reactions" of the system. No quenching by Rh(I) is detected at pH 8 at 10^{-4} M, a level typical of that produced in the absence of added platinum. Quenching rate constants for $Rh(bpy)_2Cl(H_2O)^{2+}$ and $Rh(bpy)_2Cl(OH)^+$ were determined once these complexes were suspected to be present as impurities in solutions of $Rh(bpy)_2(H_2O)_2^{3+}$ and $Rh(bpy)_2(OH)_2^+$. Since the rate constants for the monochloro complexes are so high (Table IV), relatively small levels of these increased the apparent quenching efficiencies of $Rh(bpy)_2(H_2O)_2^{3+}$ by ~100% and of $Rh(bpy)_2(OH)_2^+$ by 1 order of magnitude or more, depending on the identity of $*RuL_3^{2+}$.

Three processes must be considered as possible pathways for quenching of the $*RuL_3^{2+}$ emission by the rhodium complexes. These involve electron transfer from $*RuL_3^{2+}$ to Rh(III), electron transfer from Rh(III) to $*RuL_3^{2+}$, and energy transfer from $*RuL_3^{2+}$ to Rh(III).[1,19] The rate constants for electron-transfer quenching and energy-transfer quenching are a function of the oxidation–reduction potentials and the spectroscopic properties, respectively, of the reaction partners. The excited-state energies relevant to energy-transfer quenching are ~2.1 eV for RuL_3^{2+}[15] and ~2.75 eV for $Rh(phen)_3^{3+}$ or $Rh(bpy)_3^{3+}$.[24] Thus energy transfer from the RuL_3^{2+} excited states to $Rh(phen)_3^{3+}$ or $Rh(bpy)_3^{3+}$ is likely to be very slow ($\ll 10^7$ M^{-1} s^{-1}) since it is an uphill process. In addition, electron-transfer quenching involving formation of RuL_3^+ and Rh(IV) should also be very slow since $E°$ for the Rh(IV)/Rh(III) couple is >+1.5 V while the $E°$ values for the $*RuL_3^{2+}/RuL_3^+$ couples do not exceed +1 V.[1] Energy-transfer quenching is not ruled out for $Ru(bpy)_2(H_2O)_2^{3+}$ and $Rh(bpy)_2(OH)_2^+$, and we shall return to this point later. By elimination it seems likely that $Rh(phen)_3^{3+}$ and $Rh(bpy)_3^{3+}$ quench by oxidizing $*RuL_3^{2+}$ to give RuL_3^{3+} and a Rh(II) complex. The excited-state $*E°$ values for the $RuL_3^{3+}/*RuL_3^{2+}$ couples relevant to this process are included in Table III. We turn now to the question of the $E°$ values for the Rh(III)/Rh(II) couples.

Table V. Voltammetric Data for the Rhodium Complexes at 25 °C in Aqueous Solutions

v, V s^{-1}	E_{pc}, V (i_{pc}, μA)		E_{pa}, V(i_{pa}, μA)
	$Rh(phen)_3^{3+}$ [a]		
0.20	−0.725 (−39.2)[e]	−0.948 (−111.0)	0.012 (26.0)[g]
0.10	−0.708 (−23.3)[e]	−0.931 (−80.5)	0.005 (20.7)[g]
0.05	[f]	−0.918 (−58.0)	−0.001 (15.5)[g]
0.02	[f]	−0.903 (−37.2)	−0.014 (10.0)[g]
0.01	[f]	−0.889 (−26.0)	−0.028 (6.3)[g]
	$Rh(bpy)_3^{3+}$ [b]		
0.20		−0.782 (−46.3)	−0.140 (28.8)
0.10		−0.772 (−33.8)	−0.158 (20.0)
0.05		−0.761 (−24.0)	−0.178 (14.0)
0.02		−0.748 (−15.3)	−0.196 (8.6)
0.01		−0.739 (−10.4)	−0.211 (6.1)
	cis-$Rh(bpy)_2(OH)_2^+$ [c]		
0.20	−0.698 (−1.29)[e]	−1.006 (−83.5)	−0.133 (27.2)
0.10	−0.683 (−0.67)[e]	−0.993 (−59.0)	−0.151 (19.3)
0.05	−0.673 (−0.39)[e]	−0.980 (−42.5)	−0.165 (13.9)
0.02	−0.660 (−0.18)[e]	−0.965 (−27.0)	−0.181 (9.5)
0.01	−0.655 (−0.13)[e]	−0.954 (−19.0)	−0.192 (7.2)
	$Rh(bpy)_2^+$ [d]		
0.20			−0.070 (61.7)
0.10			−0.081 (44.2)
0.05			−0.093 (31.7)
0.02			−0.108 (19.4)
0.01			−0.120 (12.9)

[a] 2.0×10^{-3} M $Rh(phen)_3^{3+}$ in 0.05 M NaOH; sweep range +0.24 to −1.01 V. [b] 2.0×10^{-3} M $Rh(bpy)_3^{3+}$ in 0.05 M NaOH; sweep range +0.24 to −0.96 V. [c] 2.0×10^{-3} M *cis*-$Rh(bpy)_2(OH)_2^+$ in 0.05 M NaOH; sweep range +0.24 to −1.06 V. [d] 2.0×10^{-3} M *cis*-$Rh(bpy)_2(OH)_2^+$ in 0.05 M NaOH reduced at −0.96 V to generate $Rh(bpy)_2^+$; sweep range +0.34 to −0.56 V. [e] Shoulder. [f] Unresolved shoulder between −0.70 and −0.75 V. [g] An unresolved anodic shoulder was observed between −0.25 and −0.31 V.

Reduction Potentials of the Rh(III) Complexes. Kew, DeArmond, and Hanck characterized the electrochemical behavior of the bpy and phen complexes of Rh(III) on platinum in acetonitrile.[25,26] For $Rh(phen)_3^{3+}$, $Rh(phen)_2(bpy)^{3+}$, and $Rh(phen)(bpy)_2^{3+}$, they observed a quasi-reversible, one-electron cathodic wave at −0.7 to −0.9 V vs. SCE. The electron transfer was followed by a chemical reaction (possibly ligand loss) with a rate constant of ~0.1 s^{-1}.[26] A second cathodic wave ~0.1 V negative of the first was followed by rapid chemical reaction. The two one-electron-transfer processes are reasonably ascribed to reduction of Rh(III) to Rh(II) and reduction of Rh(II) to Rh(I), respectively. The behavior of $Rh(bpy)_3^{3+}$ was similar except that the reaction following the first electron transfer was very rapid. In order to clarify the thermodynamics of the various Rh(III)/Rh(II) couples in aqueous solutions, we carried out cyclic voltammetry of 2.0×10^{-3} M $Rh(phen)_3^{3+}$, *cis*-$Rh(bpy)_2(OH)_2^+$, and $Rh(bpy)_3^{3+}$ on a pyrolytic graphite electrode in aqueous 0.05 M NaOH at 25 °C. The results of these measurements are summarized in Table V.

The cyclic voltammetry of $Rh(phen)_3^{3+}$ is simpler than that of the other complexes and so is considered first. Voltammograms obtained for $Rh(phen)_3^{3+}$ (Figure 2) showed no reversible features when the sweep range was from +0.24 to −1.06 V with a sweep rate of 200 mV s^{-1}. If, however, the sweep direction was reversed at −0.76 V, the anodic partner of the −0.703-V reduction wave was detected at −0.633 V. The anodic wave became more prominent at faster sweep rates although the peak current for the

(22) Bolletta, F.; Maestri, M.; Moggi, L.; Balzani, V. *J. Phys. Chem.* **1974**, *78*, 1374.
(23) Demas J. N.; Addington, J. W.; Peterson, S. H.; Harris, E. W. *J. Phys. Chem.* **1977**, *81*, 1039.
(24) Carstens, D. H. W.; Crosby, G. A. *J. Mol. Spectrosc.* **1970**, *34*, 113.
(25) Kew, G.; DeArmond, K.; Hanck, K. *J. Phys. Chem.* **1974**, *78*, 727.
(26) Kew, G.; Hanck, K.; DeArmond, K. *J. Phys. Chem.* **1975**, *79*, 1829.

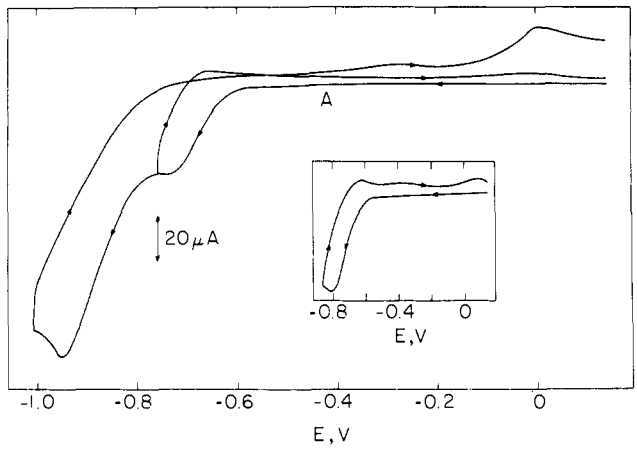

Figure 2. Cyclic voltammograms of $Rh(phen)_3^{3+}$ (2.0×10^{-3} M) in 0.05 M NaOH at 25 °C obtained at 0.2 V s^{-1} and (insert) at 5 V s^{-1}.

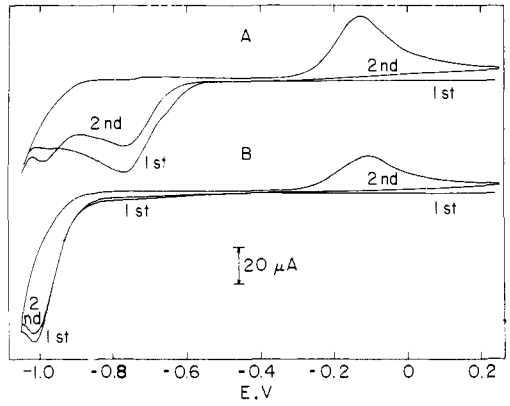

Figure 3. Cyclic voltammograms at 0.2 V s^{-1} obtained for A, $Rh(bpy)_3^{3+}$ (2.0×10^{-3} M), and B, *cis*-$Rh(bpy)_2(OH)_2^+$ (2.0×10^{-3} M), in 0.05 M NaOH at 25 °C.

anodic wave (i_{pa}) was less than the peak current for the cathodic wave (i_{pc}), even at 5 V s^{-1} (insert in Figure 2). This behavior is ascribed to reduction of $Rh(phen)_3^{3+}$ followed by chemical reaction of the reduction product. A one-electron-transfer process is implicated on the basis of the parameters obtained: the peak-to-peak separation ($E_{pa} - E_{pc}$ = 0.08 V) and the peak-to-half-peak separation ($E_{(p/2)c} - E_{pc}$ = 0.060 V) are consistent with reversible one-electron transfer.[27] Furthermore, the magnitude of i_{pc} is 97% as great as that observed for one-electron reversible oxidation of $Ru(bpy)_3^{2+}$ at the same concentration. Thus we conclude that $E_{1/2}$ for $Rh(phen)_3^{3+}/Rh(phen)_3^{2+}$ is −0.67 V under the conditions of our experiments. Preliminary results indicate the rate constant[27] for the reaction of the reduction product $Rh(phen)_3^{2+}$ to be ~30 s^{-1} (although there is some question that this process follows simple first-order kinetics). The $E_{1/2}$ for the $Rh(phen)_3^{3+}/Rh(phen)_3^{2+}$ couple was found to be −0.75 V vs. SCE in acetonitrile.[26]

Cyclic voltammograms obtained for $Rh(bpy)_3^{3+}$ are shown in Figure 3A. The small prewave at ~−0.65 V is ascribed to adsorption by analogy with that seen for $Rh(bpy)_2(OH)_2^+$ (vide infra), but quantitative analysis of its behavior was not attempted since the first cathodic wave (−0.772 V in the figure) makes a large contribution to the current in this region. In multiple sweeps, the current at −0.772 V was found to diminish as a new cathodic peak at −0.974 V grew in intensity. This is ascribed to bpy loss from $Rh(bpy)_3^{3+}$ to give $Rh(bpy)_2(OH)_2^+$. Catalysis of this process by Rh(I) (formed here as electrochemical reduction product) has already been discussed. No anodic partner to the −0.772 V peak was seen even at sweeps up to 5 V s^{-1} (in the presence or absence of 10^{-2} M added bpy). Schemes involving reversible electron transfer followed by rapid chemical reaction and irreversible electron transfer were considered. The slope of the linear plot of E_{pc} vs. ln $v^{1/2}$, where v is the sweep rate, is −0.028 ± 0.002 V, in good agreement with the theoretical value −0.026 V for reversible electron transfer followed by chemical reaction.[27] The value of $E_{pc} - E_{(p/2)c}$, which should be independent of sweep rate for irreversible electron transfer, is markedly sweep-rate dependent. Thus it is concluded that $Rh(bpy)_3^{3+}$ is reversibly reduced to $Rh(bpy)_3^{2+}$ and that the reduction product $Rh(bpy)_3^{2+}$ reacts rapidly to give a species which is electrode inactive at that potential. The fact that no anodic partner to the Rh(III)/Rh(II) reduction wave is seen at sweep rates up to 200 V s^{-1} leads to the conclusion that the rate constant for the reaction[28] of $Rh(bpy)_3^{2+}$ must exceed 300 s^{-1} (if the reaction is first order in $Rh(bpy)_3^{2+}$). Although no second reduction peak ascribable to the $Rh(bpy)_3^{2+}/Rh(bpy)_3^+$ couple is observed in aqueous solution, the shape and integrated current found for the cathodic $Rh(bpy)_3^{3+}$ wave in initial scans indicate that reduction of Rh(II) to Rh(I) occurs in the range −0.8 to −1.0 V. Since $n = 1$ for the peak, $E_{1/2}$ for the Rh(II)/Rh(I) couple is probably at least 0.1 V more negative than that for Rh(III)/Rh(II). Although neither $E_{1/2}$ value can be directly evaluated from the present results because of the rapidity of the subsequent chemical reactions, estimates may be obtained by comparison with the results obtained in acetonitrile. $E_{1/2}$ values of ~−0.8 and −0.75 V vs. SCE were obtained for $Rh(bpy)_3^{3+}/Rh(bpy)_3^{2+}$ and $Rh(phen)_3^{3+}/Rh(phen)_3^{2+}$, respectively, in acetonitrile.[25,26] In aqueous solution, $E_{1/2}$ for $Rh(phen)_3^{3+}/Rh(phen)_3^{2+}$ is −0.67 V. Since the solvent dependence of $E°$ values for $M(phen)_3^{3+}/M(phen)_3^{2+}$ couples is small,[29] the difference between the $E_{1/2}$ values for the phen and bpy couples is likely to be the same in water as in acetonitrile. On this basis $E_{1/2}$ for the $Rh(bpy)_3^{3+}/Rh(bpy)_3^{2+}$ couple is calculated to be −0.72 V in water. Thus $E_{1/2}$ values for $Rh(bpy)_3^{3+}/Rh(bpy)_3^{2+}$ and $Rh(bpy)_3^{2+}/Rh(bpy)_3^+$ are estimated as −0.7 and ≤−0.8 V, respectively, in aqueous solution.

A cyclic voltammogram obtained for $Rh(bpy)_2(OH)_2^+$ at a sweep of 100 mV s^{-1} is shown in Figure 3B. The small shoulder at ~−0.7 V is ascribed to an adsorption wave since plots of current vs. sweep rate for this "peak" are linear.[27] The electrochemical redox process starts from the next (more negative) peak observed at −0.993 V at 100-mV s^{-1} sweep. Since no anodic partner for this peak was detected under any conditions a simple reversible electron-transfer scheme is not applicable. Two alternative schemes, reversible electron transfer followed by rapid chemical reaction and irreversible electron transfer, were again considered. The slope −0.035 V obtained from a linear plot of E_{pc} vs. ln $v^{1/2}$ is consistent with an irreversible two-electron transfer with α = 0.38; the value of $E_{pc} - E_{(p/2)c}$ is −0.056 ± 0.005 V in the sweep range 0.01–0.2 V s^{-1}, consistent with a two-electron reduction with n = 0.43;[27] the slope of the linear ln i_{pc} vs. E_{pc} plot gives α = 0.37 for two-electron transfer.[27] Finally, the magnitude of i_{pc} is 2.2 ± 0.2 times greater than the value obtained for reversible one-electron oxidation of $Ru(bpy)_3^{2+}$ at the same concentration,

(27) Nicholson, R. S.; Shain, I. *Anal. Chem.* **1964**, *36*, 706.

(28) The nature of the electroinactive product of $Rh(bpy)_3^{2+}$ reaction is of some interest. The species $Rh(bpy)_2^{2+}$ resulting from bpy loss can be ruled out: loss of bpy from $Rh(bpy)_3^{2+}$ is rather slow (k = 0.5–1.0 s^{-1},[9] vide infra). Furthermore, bpy loss would be suppressed by the addition of bpy, yet added bpy was observed to produce no change in the cyclic voltammograms of $Rh(bpy)_3^{3+}$. The formation of a *monodentate* $Rh(bpy)_3^{2+\prime}$ species is a possibility: dissociation of one pyridine group from $Rh(bpy)_3^{2+}$ could be rapid and such a process would not be affected by added bpy. The fact that no anodic wave is seen for the tris species would require that the equilibrium between $Rh(bpy)_3^{2+}$ and $Rh(bpy)_3^{2+\prime}$ lie on the side of $Rh(bpy)_3^{2+\prime}$ ($K \geq 10$). In addition, the fact that no evidence for oxidation of $Rh(bpy)_3^{2+\prime}$ to the analogous Rh(III) complex $Rh(bpy)_3^{3+\prime}$ is seen below ~0.0 V would require that the monodentate Rh(III) complex be very unstable with respect to its tris form ($K = 10^{-7}$ if $K = 10$ for the equilibrium on Rh(II)). An alternative explanation for our failure to observe $Rh(bpy)_3^{2+}$ oxidation involves, not substitution, but rapid disproportionation, i.e., $2Rh(bpy)_3^{2+} \rightleftharpoons Rh(bpy)_3^{3+} + Rh(bpy)_3^+$ and $Rh(bpy)_3^+ \xrightarrow{\text{fast}} Rh(bpy)_2^+ + bpy$. Yet another alternative—that reduction first occurs at the ligand to give $Rh^{III}(bpy)_2(bpy^-)^{2+}$ (followed by intramolecular electron transfer from bpy^- to the metal)—seems unlikely: the $Rh(bpy)_3^{2+}$ product of flash-photolysis and pulse-radiolysis experiments does not absorb significantly in the visible spectra (ref 9 and Schwarz, H. A., unpublished observations) and thus lacks the characteristic bpy^- chromophore.

(29) Mayer, U.; Kotocova, A.; Gutmann, V. *J. Electroanal. Chem.* **1979**, *103*, 409.

consistent with $\alpha = 0.47$ for two-electron reduction of $Rh(bpy)_2(OH)_2^+$.[27] In short, the reduction of $Rh(bpy)_2(OH)_2^+$ in 0.05 M NaOH involves irreversible two-electron reduction of Rh(III) to Rh(I) at ~−0.95 V. No reversible one-electron process involving Rh(III) and Rh(II) is observed, but $E_{1/2}$ for the latter couple is presumably more negative than ~−0.95 V.

Results obtained for cyclic voltammetry of Rh(I) solutions prepared by controlled potential electrolysis of *cis*-$Rh(bpy)_2(OH)_2^+$ are also included in Table V. Here again the behavior implicates an irreversible two-electron transfer process (oxidation of Rh(I) to Rh(III)). A linear plot of E_{pa} vs. $\ln v^{1/2}$ gives a slope of 0.033 V consistent with irreversible two-electron transfer ($\alpha = 0.40 \pm 0.05$). A slope of 31.5 V^{-1} is obtained from the plot of $\ln i$ vs. E_{pa}, indicating $\alpha = 0.4$ for irreversible two-electron transfer. The anodic peaks obtained from cyclic voltammetry of $Rh(bpy)_3^{3+}$ and *cis*-$Rh(bpy)_2(OH)_2^+$ are similar to (but not identical with) those obtained for Rh(I) oxidation, perhaps reflecting the complicated equilibria involving Rh(I).

Quenching Mechanisms. Having estimated $E°$ values of −0.67 V for $Rh(phen)_3^{3+}/Rh(phen)_3^{2+}$, −0.7 V for $Rh(bpy)_3^{3+}/Rh(bpy)_3^{2+}$, and <−0.95 V for $Rh(bpy)_2(OH)_2^+/Rh(bpy)_2(OH)_2$, we reconsider the quenching data in Table III. For $Rh(phen)_3^{3+}$ and $Rh(bpy)_3^{3+}$ the rate constants increase slightly as the reduction potential for the $RuL_3^{3+}/{}^*RuL_3^{2+}$ couple becomes more negative, ranging from 4.1×10^8 M^{-1} s^{-1} for L = 5-Cl(phen) ($*E° = -0.77$ V[15]) to 1.3×10^9 M^{-1} s^{-1} for L = 4,7-$(CH_3)_2$(phen) ($*E° = -1.01$ V).[15] This reactivity pattern suggests[15] that the quenching mechanism involves electron transfer from $*RuL_3^{2+}$ to $Rh(phen)_3^{3+}$ or $Rh(bpy)_3^{3+}$, giving RuL_3^{3+} and $Rh(phen)_3^{2+}$ or $Rh(bpy)_3^{2+}$ as products. The reduction potentials determined for $Rh(phen)_3^{3+}$ and $Rh(bpy)_3^{3+}$ indicate that this is indeed a thermodynamically favorable process with the driving force spanning the range ~0.1–0.3 V over the $*RuL_3^{2+}$ complexes studied. Furthermore the detailed dependence of k_q on $*E°$ for either Rh(III) complex is similar to that found for other systems.[30] We were unable to obtain $E°$ data for $Rh(bpy)_2(H_2O)_2^{3+}$. However, the close parallel between k_q values for $Rh(bpy)_3^{3+}$ and $Rh(bpy)_2(H_2O)_2^{3+}$ suggests that the latter also quenches by electron transfer and that the $E°$ for the $Rh(bpy)_2(H_2O)_2^{3+}/Rh(bpy)_2(H_2O)_2^{2+}$ couple is similar to that for the tris(bipyridine) couple. On the other hand, E° for the dihydroxy couple is very negative, and electron transfer from $*RuL_3^{2+}$ to $Rh(bpy)_2(OH)_2^+$ should be uphill for most of the $*RuL_3^{2+}$ couples and consequently rather slow. The quenching rate contants range from 0.1×10^8 to 0.2×10^8 M^{-1} s^{-1}. This small range is not consistent with an electron-transfer quenching mechanism: since the quenching rates are well below the diffusion-controlled limit, the rate constants should change by a factor of at least 10^2 for the range of $*RuL_3^{2+}$ complexes used. A possible explanation for the very small free-energy dependence of the $Rh(bpy)_2(OH)_2^+$ quenching constants is that the reactions proceed predominantly by energy rather than by electron transfer: only a very small variation in rate constants is expected for the former quenching mechanism.[15,30] This interpretation seems reasonable since the absorption by $Rh(bpy)_2(OH)_2^+$ extends to lower energies than the absorption by the other Rh(III) complexes studied.

Flash Photolysis: Formation of Rh(II). Electron transfer from $*RuL_3^{2+}$ to Rh(III) has been proposed as the quenching mechanism for $Rh(phen)_3^{3+}$, $Rh(bpy)_3^{3+}$, and $Rh(bpy)_2(H_2O)_2^{3+}$. For $Ru(bpy)_3^{2+}$ this mechanism was confirmed by flash-photolysis experiments. Solutions of $Ru(bpy)_3^{2+}$ and $Rh(bpy)_3^{3+}$ were excited with a ~20-ns pulse of 530-nm light and monitored at 450 nm.[9] Only bleaching, corresponding first to $*Ru(bpy)_3^{2+}$ formation and later to $Ru(bpy)_3^{3+}$ formation, was observed. On the basis of the magnitude of the bleaching observed for a $Ru(bpy)_3^{2+}/Fe^{3+}$ solution in 0.5 M H_2SO_4 ($\Phi_{Ru(III)} = 0.9 \pm 0.1$[31-33]), the yield of $Ru(bpy)_3^{3+}$ for $Rh(bpy)_3^{3+}$ as quencher is 0.15 ± 0.03. For $Rh(bpy)_3^{3+}$ this yield was the same, within experimental error, in 0.5 M H_2SO_4, 0.17 M Na_2SO_4 (pH 8.0), and 0.4 M TEOA (pH 7, with and without 3×10^{-3} M bpy). For the 0.5 M H_2SO_4 medium the restoration of the 450-nm absorbance was followed into the millisecond time region. Analysis of the absorbance–time profile gave a rate constant of 3×10^9 M^{-1} s^{-1} for the "back-reaction" of $Ru(bpy)_3^{3+}$ and $Rh(bpy)_3^{2+}$ to form $Ru(bpy)_3^{2+}$ and $Rh(bpy)_3^{3+}$. The large magnitude of this rate constant strongly suggests that the yield of free $Ru(bpy)_3^{3+}$ in the system is limited by the cage escape yield,[17] i.e., by the ratio $k_{34}/(k_{30} + k_{34})$ in eq 12.

$$*Ru(bpy)_3^{2+} + Rh(bpy)_3^{3+} \rightleftharpoons *Ru(bpy)_3^{2+}|Rh(bpy)_3^{3+} \quad (12a)$$

$$*Ru(bpy)_3^{2+}|Rh(bpy)_3^{3+} \rightleftharpoons Ru(bpy)_3^{3+}|Rh(bpy)_3^{2+} \quad (12b)$$

$$Ru(bpy)_3^{3+}|Rh(bpy)_3^{2+} \xrightleftharpoons{k_{34}} Ru(bpy)_3^{3+} + Rh(bpy)_3^{2+} \quad (12c)$$

$$\downarrow k_{30}$$

$$Ru(bpy)_3^{2+}|Rh(bpy)_3^{3+} \rightleftharpoons Ru(bpy)_3^{2+} + Rh(bpy)_3^{3+} \quad (12d)$$

The basic form of triethanolamine has been shown to reduce $Ru(bpy)_3^{3+}$ to $Ru(bpy)_3^{2+}$ [3,8] evidently producing a radical cation $TEOA^+$. Kalyanasundaram, Kiwi, and Grätzel[3] found that $TEOA^+$ could act as an oxidant or rearrange to a species with reducing properties. Kirch, Lehn, and Sauvage[8] have proposed that this rearranged TEOA radical reduces $Rh(bpy)_3^{2+}$ to $Rh(bpy)_3^+$. In order to clarify the role of the TEOA radical(s) in the present system, we carried out flash- and continuous-photolysis experiments on the MV^{2+}, $Ru(bpy)_3^{2+}$, TEOA system. A quenching rate constant of 1.4×10^9 M^{-1} s^{-1} for eq 13 was determined in a sodium sulfate medium ($\mu = 0.5$ M, 25 °C). In flash-photolysis experiments in which the MV^+ absorption at 605 nm was monitored, we found, in accord with previous studies,[3] that MV^+ appeared in two stages. At pH 7–9 the first increment appeared in parallel with $Ru(bpy)_3^{3+}$ by reaction 13 with a pH-independent rate. At constant total TEOA concentration, the rate and magnitude of the second slower stage appeared to depend on pH as reported in ref 3. More detailed studies, however, revealed two features not noted in the previous report. First, in 0.1 M TEOA at pH 7 and in 0.2 M TEOA at pH 8, the rate of "delayed" MV^+ appearance was independent of MV^{2+} ($(0.6–4.5) \times 10^{-3}$ M). Secondly, the rate of the delayed stage, at a given pH, was a function of the TEOA level. All of the rate data in the pH range 7–9 are, in fact, compatible with a rate that is first order in the radical and first order in unprotonated TEOA ($pK_a = 8.1$) with a rate constant of $(3.3 \pm 0.5) \times 10^6$ M^{-1} s^{-1} at 25 °C. The following scheme (eq 14–18) is consistent with the above observations. The rate constants determined for the individual steps are $k_{14} = 0.2 \times 10^8$ M^{-1} s^{-1},[9] $k_{15} = 4.4 \times 10^9$ M^{-1} s^{-1}, $k_{17} = (3.3 \pm 0.5) \times 10^6$ M^{-1} s^{-1}, $k_{18} > 10^8$ M^{-1} s^{-1}, and a cage escape yield (eq 13) of 0.25 ± 0.05. The value of k_{16}/k_{17} was found to be $\sim 10^3$ from the MV^+ absorbance–time profiles for flash- and continuous-photolysis experiments carried out at known light intensity. In eq 17, the TEOA-assisted rearrangement of the oxidizing $TEOA^+\cdot$ to its reducing form $TEOA'\cdot$ is written as H atom abstraction from TEOA by analogy with the pathway found in the triethylamine cation radical system.[34] Thus when k_{17}[TEOA]

$$Ru(bpy)_3^{3+} + TEOA \rightarrow Ru(bpy)_3^{2+} + TEOA^+\cdot \quad (14)$$

$$Ru(bpy)_3^{3+} + MV^+ \rightarrow Ru(bpy)_3^{2+} + MV^{2+} \quad (15)$$

$$TEOA^+\cdot + MV^+ \rightarrow TEOA + MV^{2+} \quad (16)$$

$$TEOA^+\cdot + TEOA \rightarrow TEOAH^+ + TEOA'\cdot \quad (17)$$

$$TEOA'\cdot + MV^{2+} \rightarrow \text{products} + MV^+ \quad (18)$$

(30) Brunschwig, B. S.; Sutin, N. *J. Am. Chem. Soc.* **1978**, *100*, 7568.
(31) Lin, C.-T.; Sutin, N. *J. Phys. Chem.* **1976**, *80*, 97.
(32) Taylor, D. G.; Demas, J. N. *J. Chem. Phys.* **1979**, *7*, 1032.
(33) Bolletta, F.; Juris, A.; Maestri, M.; Sandrini, D. *Inorg. Chim. Acta* **1980**, *44*, L175.
(34) DeLaive, P. J.; Whitten, D. G.; Gianotti, C. *Adv. Chem. Ser.* **1979**, *No. 173*, 234.

$\gg k_{16}[MV^+]$, the oxidizing radical $TEOA^{+\cdot}$ is converted quantitatively to $TEOA'\cdot$ ($(HOCH_2CH_2)_2\dot{N}CHCH_2OH$ or $(HOCH_2CH_2)_2NCH_2\dot{C}HOH$) which rapidly reduces MV^{2+} to MV^+, and the ratio of MV^+ formed per $Ru(bpy)_3^{3+}$ in eq 13 is 2.0.

As in the above sequence, $Ru(bpy)_3^{3+}$ produced by reaction of $*Ru(bpy)_3^{2+}$ and $Rh(bpy)_3^{3+}$ (eq 12) is reduced by TEOA (eq 14). Although oxidation of Rh(II) (and Rh(I)) by $TEOA^+$ is probably very rapid ($k > 10^9$ M^{-1} s^{-1}), rearrangement of $TEOA^{+\cdot}$ by H atom abstraction from TEOA to give $TEOA'\cdot$ predominates at the high [TEOA] used in our studies. In contrast to the proposal of Kirch, Lehn, and Sauvage[8] that the $TEOA'\cdot$ reduces $Rh(bpy)_3^{2+}$ to $Rh(bpy)_3^+$, our observations[9] strongly suggest that the $TEOA'\cdot$ reduces $Rh(bpy)_3^{3+}$ to $Rh(bpy)_3^{2+}$. We have found that a nearly colorless ($\epsilon < 10^{-3}$ M^{-1} cm^{-1} at $\lambda = 450$–600 nm) reduced rhodium complex is present within ~ 0.5 μs of the flash in a solution containing 3×10^{-5} M $Ru(bpy)_3^{2+}$, 5×10^{-3} M $Rh(bpy)_3^{3+}$, and 0.1 M TEOA at pH 8.1 and reduces MV^{2+} with a rate constant of $(4 \pm 1) \times 10^8$ M^{-1} s^{-1}.[9] As the quantum yield of MV^+ observed here is 0.33 ± 0.04, either 1 $Rh(bpy)_3^+$ or 2 $Rh(bpy)_3^{2+}$ per $Ru(bpy)_3^{3+}$ in eq 12 must be present in the system at this time. The fact that MV^+ formation is exponential when the concentration of initial photoproducts (eq 12) is only $\sim 10^{-6}$ M would require that $TEOA'\cdot$ reduce $Rh(bpy)_3^{2+}$ with a rate constant considerably exceeding 10^{10} M^{-1} s^{-1}. By contrast, the rate constant for $TEOA'\cdot$ reduction of $Rh(bpy)_3^{3+}$ to $Rh(bpy)_3^{2+}$ need only be $>10^7$ M^{-1} s^{-1} if it is $Rh(bpy)_3^{2+}$ which reduces the added MV^{2+}. The latter interpretation is obviously preferable: in the electrochemical studies it was shown that the reduction potential for the $Rh(bpy)_3^{2+}/Rh(bpy)_3^+$ couple is ≥ 0.1 V more negative than that of the $Rh(bpy)_3^{3+}/Rh(bpy)_3^{2+}$ couple. Thus, on the basis of thermodynamics, the rate constant for reduction of $Rh(bpy)_3^{2+}$ by $TEOA'\cdot$ is expected to be somewhat *smaller* than that for $Rh(bpy)_3^{3+}$ reduction. In summary, we infer that, under typical flash-photolysis conditions, the net change effected within <25 μs of the excitation pulse is

$$2Rh(bpy)_3^{3+} + TEOA \rightarrow 2Rh(bpy)_3^{2+} + \text{products} \quad (19)$$

with the quantum yield for $Rh(bpy)_3^{2+}$ being 0.3 ± 0.1, twice the cage escape yield for eq 12.

Fate of Rh(II). The quantum yield for the ultimate rhodium protoproduct Rh(I) was found to be 0.13. This suggests that $Rh(bpy)_3^{2+}$ disproportionates to Rh(I) and Rh(III). Rhodium(I) formation (520 nm) was monitored following excitation of solutions containing 5×10^{-4} M $Ru(bpy)_3^{2+}$, 5×10^{-3} M $Rh(bpy)_3^{3+}$, and 0.2 M TEOA at pH 8 and was observed to be exponential with $k_{obsd} = 2 \pm 1$ s^{-1} at 25 °C.[9] Earlier, on the basis of this observation and the results of pulse-radiolysis experiments, we postulated that loss of bpy from $Rh(bpy)_3^{2+}$ (eq 20) is rate determining ($k_{20} =$

$$Rh(bpy)_3^{2+} \rightleftharpoons Rh(bpy)_2^{2+} + bpy \quad (20)$$

$$Rh(bpy)_3^{2+} + Rh(bpy)_2^{2+} \rightarrow Rh(bpy)_3^{3+} + Rh(bpy)_2^+ \quad (21)$$

1.0 ± 0.5 s^{-1}) and is followed by rapid reduction of the $Rh(bpy)_2^{2+}$ species by $Rh(bpy)_3^{2+}$ (eq 21).[9] Recently we have been able to investigate reaction 21 directly. Solutions containing $Ru(bpy)_3^{2+}$, $Rh(bpy)_3^{3+}$, $Rh(bpy)_2(OH)_2^+$, and TEOA were monitored at 520 nm after excitation with the 20-ns pulse of 530-nm light. Here the absorbance increase characteristic of Rh(I) formation was observed to occur on the time scale of 0.1–1 ms rather than 0.1–1 s as seen in the absence of $Rh(bpy)_2(OH)_2^+$. (No Rh(I) formation was observed when the $Rh(bpy)_3^{3+}$ was omitted.) Furthermore, the Rh(I) formation was not exponential under these conditions; instead plots of $1/\Delta A_{520}$ (the reciprocal of the 520-nm absorbance increase) vs. time were linear. The slopes (k_{exptl}/ϵ) of these plots were a sensitive function of the relative amounts of $Rh(bpy)_3^{3+}$ and $Rh(bpy)_2(OH)_2^+$ present in the solution (Table VI), suggesting that the preequilibrium (22) is relevant. In eq 22, $Rh(bpy)_3^{2+}$

$$Rh(bpy)_3^{2+} + Rh(bpy)_2(OH)_2^+ \rightleftharpoons Rh(bpy)_3^{3+} + Rh(bpy)_2^{2+} + 2OH^- \quad (22)$$

produced from the quenching of $Ru(bpy)_3^{2+}$ (eq 12) reduces

Table VI. Values of k_{exptl}/ϵ Observed for Rhodium(I) Formation in Mixtures of $Rh(bpy)_3^{3+}$ and $Rh(bpy)_2(OH)_2^+$ [a]

$10^3 \times$ $[Rh(bpy)_3^{3+}]$, M	$10^3 \times$ $[Rh(bpy)_2(OH)_2^+]$, M	$[Rh(bpy)_2(OH)_2^+]/[Rh(bpy)_3^{3+}]$	$10^{-4} \cdot k_{exptl}/\epsilon$, $cm\ s^{-1}$
0	10.0		0
7.6	0		0
7.6	0.365	0.048	2.94
7.6	0.73	0.096	5.76
7.6	1.10	0.144	11.3
7.14	2.73	0.383	11.7
6.66	5.75	0.863	12.4
6.26	8.39	1.34	9.3

[a] $[Ru(bpy)_3^{2+}] = 5 \times 10^{-5}$ M, 0.2 M TEOA/$TEOAH^+$ sulfate medium at pH 8.1 and 25 °C. Values of k_{exptl}/ϵ were obtained from the slopes of plots of $1/\Delta A_{520}$ vs. time.

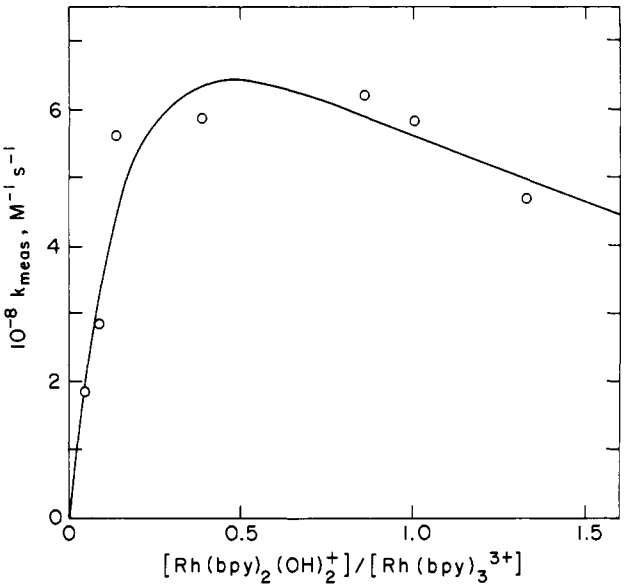

Figure 4. Plot of k_{exptl}/ϵ vs. $[Rh(bpy)_2(OH)_2^+]/[Rh(bpy)_3^{3+}]$ in a 0.2 M TEOA/$TEOAH^+$ sulfate medium at pH 8.1 and 25 °C.

$Rh(bpy)_2(OH)_2^+$ to give a bis(bipyridine)rhodium(II) complex (written here and in eq 20–22, for simplicity, as $Rh(bpy)_2^{2+}$). It will be recalled that at pH 8, $Rh(bpy)_2(OH)_2^+$ quenches only very poorly (Figure 1) so that any $Rh(bpy)_2^+$ present in the solution must arise from reactions of $Rh(bpy)_3^{2+}$. Treatment of reaction 22 as a *rapid* preequilibrium, with eq 21 rate determining in these mixtures, is suggested by the data in Table VI: values of k_{exptl}/ϵ rise sharply with $C = [Rh(bpy)_2(OH)_2^+]/[Rh(bpy)_3^{3+}]$, then level off, and drop slightly when $C > 1$. For eq 22 a rapid preequilibrium and eq 21 the rate-determining step, k_{exptl} is given by eq 23. Values of k_{exptl} were calculated from k_{exptl}/ϵ by using $\epsilon =$

$$k_{exptl} = 4k_{21}K_{22}C/(1 + K_{22}C)^2 \quad (23)$$

1.0×10^4 M^{-1} cm^{-1} and plotted against C, as shown in Figure 4. The curve was constructed by using $k_{21} = 0.3 \times 10^9$ M^{-1} s^{-1} and $K_{22} = 2.1$, with the latter parameters being determined from a plot of $(C/k_{exptl})^{1/2}$ vs. C (intercept = $1/(K_{22}k_{21})^{1/2}$, slope/intercept = K_{22}). Figure 4 shows that the relative rate of Rh(I) formation is maximal when the concentrations of $Rh(bpy)_3^{2+}$ and $Rh(bpy)_2^{2+}$ are equal as is expected for the above mechanism. We have not determined k_{22} but require that it be $>10^6$ M^{-1} s^{-1}.

Mechanism of Dihydrogen Production. $Rh(bpy)_3^{2+}$ is the product of the quenching of $*Ru(bpy)_3^{2+}$ by $Rh(bpy)_3^{3+}$, and a second equivalent of $Rh(bpy)_3^{2+}$ is formed from reduction of $Rh(bpy)_3^{3+}$ by $TEOA'$. In the absence of platinum, $Rh(bpy)_3^{2+}$ loses bpy and the product is reduced by $Rh(bpy)_3^{2+}$ to $Rh(bpy)_2^+$. Our proposed scheme for the reaction pathways occurring in the presence and absence of Pt is shown in Figure 5. Kirch, Lehn,

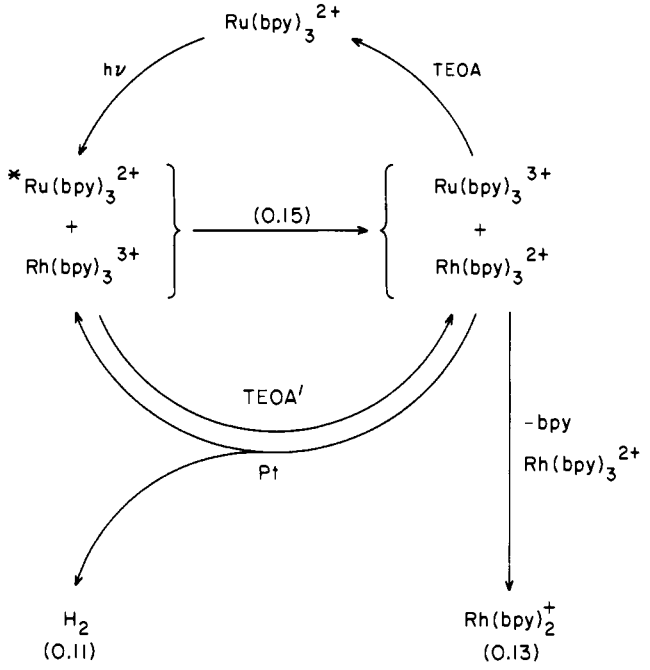

Figure 5. Outline of the reaction pathways leading to Rh(I) and H_2. The numbers in parentheses are the quantum yields for the various processes.

and Sauvage[8b] have proposed that, in the presence of platinum, Rh(I) reduces water to give H_2. We, however, have found that this is not likely: although $Rh(bpy)_3^+$ is a very strong reductant ($E° \approx -0.8$ V), the bis(bipyridine)rhodium(I) species observed in the photolysis ($E° = -0.23$ V at pH 8) is not sufficiently reducing to effect reduction of water ($E° = -0.47$ V at pH 8) to H_2; indeed Rh(I) solutions produce no detectable H_2 when left in contact with platinum for long times. On the other hand, $Rh(bpy)_3^{2+}$ ($E° = -0.7$ V) is a strong enough reductant to reduce water to H_2 under the photolysis conditions. The lifetime of $Rh(bpy)_3^{2+}$ is inherently rather long in the absence of platinum so that scavenging of $Rh(bpy)_3^{2+}$ by Pt to produce H_2 is likely to compete kinetically with the production of Rh(I). In accord with such a competition, it is observed that at low platinum, the yield of H_2 drops and Rh(I) is formed at its expense, while at high platinum no Rh(I) is observed.

To further test the notion of parallel pathways (formation of Rh(I) and scavenging by Pt to give H_2) for the consumption of Rh(II) in platinum-containing solutions, we carried out some additional experiments. In the previous section we showed that the rate of Rh(I) formation is immensely increased in the presence of $Rh(bpy)_2(OH)_2^+$. If water reduction (over platinum) by Rh(II) occurs in competition with Rh(I) formation, factors which increase the Rh(I) formation rate should diminish the rate and yield of H_2 production. The quantum yields observed for H_2 production (Table II) do exhibit such an effect ($[Rh(bpy)_2(OH)_2^+]/[Rh(bpy)_3^{3+}]$, Φ_{H_2}): 0, 0.11 mol einstein^{-1}; 0.1, 0.008 mol einstein^{-1}; 0.26, 0.000 mol einstein^{-1}; 17.5, 0.005 mol einstein^{-1}. The first three results show that as the rate of Rh(I) formation increases (see Figure 4) and the lifetime of $Rh(bpy)_3^{2+}$ decreases, the H_2 drops precipitously as is expected if it is $Rh(bpy)_3^{2+}$ which reduces water to H_2 in the presence of Pt.

The last result at very high added $Rh(bpy)_2(OH)_2^+$ is striking in another context. In this experiment H_2 was observed under conditions where the Rh(I) formation rate is rather slow because the Rh(II) is stored as a bis(bipyridine) species (equilibrium 22 lies very far to the right). The fact that H_2 is observed here indicates that the bis(bipyridine) complex (which under normal photolysis conditions could not accumulate) also reduces water to H_2 in the presence of Pt. Direct photolysis of $Rh(bpy)_2(OH)_2^+$, $Ru(bpy)_3^{2+}$, and TEOA mixtures containing Pt yields no H_2, but since $Rh(bpy)_2(OH)_2^+$ is a poor quencher (and probably quenches by energy transfer, in any case), little $Rh(bpy)_2^{2+}$ is formed under such conditions. Both the electrochemical and quenching measurements indicate that $Rh(bpy)_2^{2+}$ should be at least as strongly reducing as $Rh(bpy)_3^{2+}$. Thus (catalyzed) reduction of water by $Rh(bpy)_2^{2+}$ is quite reasonable. In summary, we conclude that under the usual photolysis conditions it is $Rh(bpy)_3^{2+}$ which is responsible for catalyzed reduction of water to H_2; when the conditions are altered so that $Rh(bpy)_2^{2+}$ replaces $Rh(bpy)_3^{2+}$ as the dominant form of Rh(II), H_2 is also produced. Factors which accelerate the conversion of Rh(II) to Rh(I) lower the yield of H_2 as is expected if reactions of Rh(II) *and not of Rh(I)* are responsible for H_2 production.

Comparisons with Other Systems. We conclude by comparing the pathways and efficiencies observed for four of the $Ru(bpy)_3^{2+}$-based systems reported to effect the photoreduction of water.[2] These include the present heterogeneous $Rh(bpy)_3^{3+}$-mediated system, the heterogeneous MV^{2+}-mediated system,[4,6] the heterogeneous Et_3N-driven system in 25% aqueous acetonitrile,[34,35] and the homogeneous $Co^{II}(Me_6[14]dieneH_4)(H_2O)_2^{2+}$-($Co^{II}L$)-mediated system.[10] The maximum hydrogen quantum yields observed for these systems are 0.11, 0.13,[4] 0.53,[35] and 0.05,[10] respectively. (The value of Φ_{H_2} for the MV^{2+} system is close to half the cage escape yield determined in this work (0.25 ± 0.05), suggesting that the radicals produced upon the reduction of EDTA at pH 5 do not yield an additional MV^+.[2]) Although all four systems run at the expense of "sacrificial" reagents (TEOA for $Rh(bpy)_3^{3+}$, EDTA for MV^{2+}, Et_3N for the nonaqueous system, and Eu(II) or ascorbate ion for $Co^{II}L$), all three can be made to effect net energy storage. The mechanisms elucidated for $Rh(bpy)_3^{3+}$ and MV^{2+} involve eq 1–5: oxidative quenching of $*Ru(bpy)_3^{2+}$ to give $Ru(bpy)_3^{3+}$ and Q^- ($Rh(bpy)_3^{2+}$ or MV^+) with a yield (ϕ_{cage}) determined by the relative rates of "back-reaction" and cage dissociation (eq 12).[36] The role of the sacrificial reagent is to suppress the diffusional back-reaction by eliminating $Ru(bpy)_3^{3+}$. (For TEOA this also leads to introduction of an additional reducing equivalent from eq 17 and 19.) The lifetimes of the strong reductants $Rh(bpy)_3^{2+}$ or MV^+ are thus prolonged so that reduction of water can be accomplished on the heterogeneous catalyst (Pt for the former and PtO_2[3] and others[4,6] for the latter). For the $Rh(bpy)_3^{2+}$ system, comparison of the observed Φ_{H_2} (0.11 ± 0.02) with the theoretical yield based on Rh(II) ((0.3 ± 0.1)/2) indicates that Pt is at least 70% efficient in channeling the Rh(II)-reducing equivalents into the desired product H_2. The quantum yield for H_2 production in this system is thus most severely limited by the cage escape yield for the early photochemical events—not by the scavenger- and catalyst-promoted dark reactions. On the basis of the data presently available, similar considerations apply to the MV^{2+} system.

The primary photochemical reaction in the heterogeneous Et_3N-driven system and in the homogeneous ascorbate- or Eu^{2+}-driven, $Co^{II}L$-mediated systems is different from the one considered above. In these systems $*Ru(bpy)_3^{2+}$ is reduced by the sacrificial reagent to give $Ru(bpy)_3^+$ with a cage escape yield of 0.5–1.0.[37,38] In the Et_3N system the $Ru(bpy)_3^+$ (or $EtN{=}CHCH_3$) reacts at the PtO_2 catalyst to produce hydrogen with a quantum yield of 0.53. The quantum yield for hydrogen production in the $Co^{II}L$ system is considerably lower: in this system

(35) DeLaive, P. J.; Sullivan, B. P.; Meyer, T. J.; Whitten, D. G. *J. Am. Chem. Soc.* **1979**, *101*, 4007.

(36) It is somewhat surprising that finite cage escape yields are obtained in these systems, considering the rapidity of the quenching reactions and the much greater exothermicity of the back-reactions. As has been previously discussed,[2] the finite cage escape yields could reflect decreased back-reaction rates resulting from the fact that the back-reactions lie in the Marcus inverted region. Another possibility is that the quenching reactions are adiabatic and the back-reactions, nonadiabatic. In the $Ru(bpy)_3^{2+}$ (and $Os(bpy)_3^{2+}$) excited state, the promoted electron is delocalized over the antibonding orbitals of the bpy^- radical anion; this could lead to good overlap with the redox orbitals of the quencher yielding an adiabatic quenching reaction. On the other hand, the back-reaction would be nonadiabatic if the Ru (or Os) t_{2g} orbitals involved in the back-reactions did not overlap very efficiently with the redox orbitals of the reduced quencher.

(37) Creutz, C.; Sutin, N. *J. Am. Chem. Soc.* **1976**, *98*, 6384.

(38) The Et_3N radical produced in the quenching step rapidly reacts with Et_3N to produce a very reducing radical.[35] As a consequence the theoretical quantum yield for H_2 formation in the Et_3N system is close to 1.0.

the $Ru(bpy)_3^+$ is used to reduce $Co^{II}L$ to a hydride which does not produce hydrogen efficiently under the *homogeneous* conditions used.

In the absence of well-defined schemes for homogeneously catalyzed reduction of water, the addition of heterogeneous catalysts such as platinum can clearly meet the need for efficient dark reactions. This study has shown that these reactions can be so efficient that the overall limiting factor in determining Φ_{H_2} is the rapidity of back-reactions tending to destroy the primary photoproducts. Factors which determine these electron-transfer rate constants include the driving force for the back-reaction,[1,39] steric factors, the charges of the reacting species, and spatial separation of the back-reactants, as well as other factors which are described in detail elsewhere.[1,40] Increased efficiency of both photochemical and dark reactions are the goals of ongoing research in this laboratory.

Acknowledgment. We thank Dr. D. Christman for performing the mass spectrometric analysis of bpy samples and Ms. E. Norton for her outstanding analytical efforts on our behalf. In addition, we gratefully acknowledge very helpful comments from Drs. G. M. Brown and H. A. Schwarz. This research was performed under the auspices of the U.S. Department of Energy and supported by its Division of Basic Energy Sciences.

(39) Creutz, C.; Sutin, N. *J. Am. Chem. Soc.* **1977**, *99*, 241.

(40) Brugger, P.-A.; Grätzel, M. *J. Am. Chem. Soc.* **1980**, *102*, 2461.

Photogeneration of Reactive $[ReH(diphos)_2]$. Its Reversible Coordination of CO_2 and Activation of Aromatic C–H Bonds

Mark G. Bradley, David A. Roberts, and Gregory L. Geoffroy*

Contribution from the Department of Chemistry, The Pennsylvania State University, University Park, Pennsylvania 16802. *Received July 14, 1980*

Abstract: Irradiation of $[ReH_3(diphos)_2]$ (diphos = $Ph_2PCH_2CH_2PPh_2$) with UV light leads to elimination of H_2 with a 366-nm quantum yield of 0.07 ± 0.02. The initial photoproduct is $[ReH(diphos)_2]$ or a solvated derivative, but this species is highly reactive and rapidly adds N_2, CO, and C_2H_4 to give the known $[ReH(N_2)(diphos)_2]$, $[ReH(CO)(diphos)_2]$, and $[ReH(C_2H_4)(diphos)_2]$ derivatives. Photolysis in the presence of C_2H_2 gives a new species tentatively formulated as $[ReH(C_2H_2)(diphos)_2]$. Irradiation in the presence of CO_2 yields the new formate complex, $[Re(O_2CH)(diphos)_2]$, which derives by reversible insertion of CO_2 into the Re–H bond of $[ReH(diphos)_2]$. NMR evidence indicates that $[ReH(diphos)_2]$ undergoes rapid but reversible ortho metalation and insertion into the C–H bonds of benzene. $[ReH(diphos)_2]$ can also be generated via photoinduced loss of N_2 from $[ReH(N_2)(diphos)_2]$.

A number of studies have demonstrated that photolysis of transition metal di- and polyhydride complexes gives elimination of H_2 as the dominant photoreaction.[1-17] Two such examples are shown in eq 1 and 2. In order to further demonstrate the

$$[IrClH_2(PPh_3)_3] \xrightarrow{h\nu} [IrCl(PPh_3)_3] + H_2 \quad (1)^4$$

$$[M(\eta^5\text{-}C_5H_5)_2H_2] \xrightarrow{h\nu} [M(\eta^5\text{-}C_5H_5)_2] + H_2 \quad (2)^{8-13}$$

$$M = Mo, W$$

generality of this type of reaction and especially to attempt to employ it for the generation of thermally unattainable reactive intermediates, we have extended our previous studies[3-8] to include several polyhydride complexes of the early transition metals. We have focused especially on Re because of the variety of known polyhydride complexes of this metal[18,19] and herein describe the results of our study of $[ReH_3(diphos)_2]$ (diphos = $Ph_2PCH_2CH_2PPh_2$).

Although the chemistry of $[ReH_3(diphos)_2]$ has not been extensively examined, the complex is known to be thermally quite stable. It shows no tendency to lose H_2 when heated to 180 °C in an evacuated Carius tube,[20] and it will not react to give the known $[ReH(N_2)(diphos)_2]$ derivative when heated under 60 psi of N_2.[21] In contrast to most metal hydrides, treatment of

(1) Geoffroy, G. L. *Prog. Inorg. Chem.* **1980**, *27*, 123.
(2) Geoffroy, G. L.; Wrighton, M. S. "Organometallic Photochemistry"; Academic Press: New York, 1979.
(3) Geoffroy, G. L.; Bradley, M. G.; Pierantozzi, R. *Adv. Chem. Ser.* **1978**, *No. 167*, 181.
(4) Geoffroy, G. L.; Pierantozzi, R. *J. Am. Chem. Soc.* **1976**, *98*, 8054.
(5) Geoffroy, G. L.; Bradley, M. G. *Inorg. Chem.* **1977**, *16*, 744.
(6) Geoffroy, G. L.; Hammond, G. S.; Gray, H. B. *J. Am. Chem. Soc.* **1975**, *97*, 3933.
(7) Pierantozzi, R.; Geoffroy, G. L. *Inorg. Chem.* **1980**, *19*, 1821.
(8) Geoffroy, G. L.; Bradley, M. G. *Inorg. Chem.* **1978**, *17*, 2410.
(9) Elmitt, K.; Green, M. L. H.; Forder, R. A.; Jefferson, I.; Prout, K. *J. Chem. Soc., Chem. Commun.* **1974**, 747.
(10) (a) Giannotti, C.; Green, M. L. H. *J. Chem. Soc., Chem. Commun.* **1972**, 1114. (b) Farrugia, L.; Green, M. L. H. *Ibid.* **1975**, 416.
(11) Berry, M.; Elmitt, L.; Green, M. L. H. *J. Chem. Soc., Dalton Trans.* **1979**, *12*, 1950.
(12) Green, M. L. H.; Berry, M.; Couldwell, C.; Prout, K. *Nouv. J. Chim.* **1978**, *2*, 13.
(13) Samat, A.; Sala-Pala, J.; Gualielmetti, R.; Guerchais, J. *Nouv. J. Chim.* **1978**, *2*, 13.
(14) Sacco, A.; Aresta, M. *J. Chem. Soc., Chem. Commun.* **1968**, 1223.
(15) Darensbourg, D. J. *Inorg. Nucl. Chem. Lett.* **1972**, *8*, 529.
(16) Ellis, J. E.; Faltynek, R. A.; Hentges, S. G. *J. Am. Chem. Soc.* **1977**, *99*, 626.
(17) Camus, A.; Cocevar, C.; Mestroni, G. *J. Organomet. Chem.* **1972**, *39*, 355.
(18) Kaesz, H. D.; Saillant, R. B. *Chem. Rev.* **1972**, *72*, 231.
(19) Giusto, D. *Inorg. Chim. Acta Rev.* **1972**, *6*, 91.
(20) Freni, M.; Demichelis, R.; Giusto, D. *J. Inorg. Nucl. Chem.* **1967**, *29*, 1433.

0002-7863/81/1503-379$01.00/0 © 1981 American Chemical Society